A Review of Recent Advances in Electrically Driven Polymer-Based Flexible Actuators: Smart Materials, Structures, and Their Applications

Junseong Ahn, Jimin Gu, Jungrak Choi, Chankyu Han, Yongrok Jeong, Jaeho Park, Seokjoo Cho, Yong Suk Oh, Jun-Ho Jeong, Morteza Amjadi,* and Inkyu Park*

Polymer-based flexible actuators have recently attracted significant attention owing to their great potentials in soft robotics, wearables, haptics, and medical devices. In particular, electrically driven polymer-based flexible actuators are considered as some of the most practical actuators because they can be driven by a simple electrical power source. Over the past decade, research on electrically driven soft actuators has greatly progressed, leading to the development of various functional materials and bioinspired structures. This article comprehensively reviews recent advances in electrically driven soft actuators and compares their actuation performance based on working principles, materials, and structures. Several strategies, including combining smart materials and composite structures, which are proposed to overcome some of the drawbacks of electrically driven soft actuators, are also discussed. Finally, potential applications of electrically driven soft actuators in soft robotics are summarized and an outlook is presented.

1. Introduction

Polymer-based flexible actuators have recently received increasing interest because of their use in robotic manipulation, artificial muscles, haptics, healthcare, and military applications.[1–3] Compared to conventional rigid actuators, polymer-based flexible actuators can safely interact with soft, curved, and even brittle objects as they are typically made of flexible and deformable materials.[4] As a result, many

researchers have been developing various types of soft actuators, including mechanically,[5–7] optically,[8,9] chemically,[10] magnetically,[11,12] and electrically[13–21] driven actuators. Among them, electrically driven actuators have attracted much attention despite their disadvantage of low blocking force, because they have merits of high design diversity, lightweight, and small size and also electric source is considered as one of the most easily accessible power sources, making them suitable for many practical applications.[13,14,22–24]

Electrically driven polymer-based flexible actuators are broadly classified as electroactive polymer (EAP) actuators and electrothermal actuators (ETAs), as shown in **Figure 1** and **Table 1**. EAP actuators utilize the direct response of active polymers under the input electric stimuli. They can be categorized as dielectric elastomer actuators (DEAs),[25–27] electroactive hydrogel (EAH) actuators,[16,28–30] and ionic polymer–metal composite (IPMC)[31,32] actuators based on the driving principle and type of the base structure. DEAs are often made of a dielectric elastomer sandwiched with two stretchable electrodes, where the actuation is controlled by an external electric field applied to the electrodes. In the cases of the EAH and IPMC actuators, ion cluster flux and electroosmotic flow of water between two electrodes (i.e., from anode to cathode) under an electric field govern the deformation of actuators, while the method of applying an electric field is slightly different for these actuators. On the other hand, the operation of ETAs is based on the Joule heating effect, resulting from the passage of an electric current through a conductor. The generated heat directly bends bilayer ETAs by the mismatch between the coefficients of thermal expansion (CTE) of two different polymers.[14,22,24,33–38] Another type of ETAs, known as thermally triggered shape memory polymer (SMP) actuators,[39–43] change their phase from a temporary shape to their original shape upon changes in their temperature.

This Review article summarizes the recent research trends in the design and development of electrically activated flexible actuators, with focus on their basic driving principles, actuating materials, and potential applications. We initially concentrate on the materials and structures employed for the development of high-performance flexible actuators. We show that several

J. Ahn, J. Gu, J. Choi, C. Han, J. Park, S. Cho, Y. S. Oh, I. Park
Department of Mechanical Engineering
Korea Advanced Institute of Science and Technology (KAIST)
Daejeon 34141, Republic of Korea
E-mail: inkyu@kaist.ac.kr
J. Ahn, Y. Jeong, J.-H. Jeong
Department of Nano Manufacturing Technology
Korea Institute of Machinery and Materials (KIMM)
Daejeon 34103, Republic of Korea
M. Amjadi
Institute of Mechanical Process and Energy Engineering
Heriot-Watt University
Edinburgh EH14 4AS, UK
E-mail: m.amjadi@hw.ac.uk

**ADVANCED
SCIENCE NEWS**
www.advancedsciencenews.com

**ADVANCED
MATERIALS
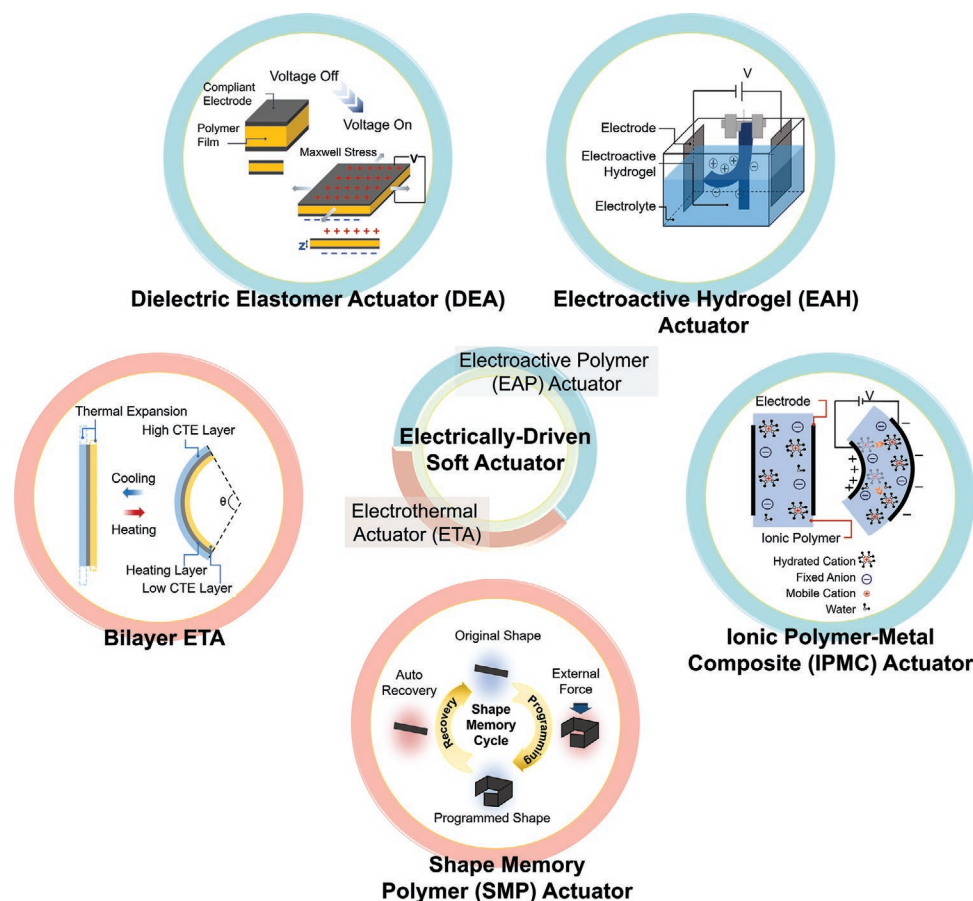TECHNOLOGIES**
www.advmattechnol.de

Figure 1. Schematic illustration of different types of electrically driven polymer-based flexible actuators. These actuators are classified into two groups depending on their working principles; electroactive polymer (EAP) actuator and electrothermal actuator (ETA). These actuators can then be categorized into five representative types depending on their working mechanisms, namely, dielectric elastomer actuators (DEAs), electroactive hydrogel (EAH) actuators, ionic polymer–metal composite (IPMC) actuators, bilayer ETA, and shape memory polymer (SMP) actuators.

strategies have recently been reported to enhance the performance of actuators by combining smart materials and composite structures. Then, the use of electrically driven soft actuators as manipulators, biomimetic robots, microfluidic valves, rehabilitation devices, and haptic devices is discussed. Finally, we discuss existing challenges and present an outlook for electrically driven soft actuators.

2. Electrically Driven Soft Actuators

2.1. EAP Actuators

EAPs are promising materials of the flexible actuators because they are lightweight and inexpensive; they change their shape and size as a function of the external electric field.[44] There are three types of EAP actuators, namely, DEAs, EAH, and IPMC. The DEAs operate based on the field-activated actuation, and typically require a high driving voltage ranging from 0.5 to 100 kV.[45,46] They show rapid response to the electrical stimulation and hold the accommodated strain under direct current (DC) conditions. In addition, they can withstand large strains over 100% and generate large blocking forces. On the other

hand, the actuation of EAH and IPMC relies on the electroresponsive charged ion migration through polymers, which leads to swelling or shrinking, and consequent changes in geometrical shape and size. The EAH and IPMC often assure long-range stroke under the applied electrical potential. However, they suffer from slow actuation and low blocking force.[47,48] Although their actuation trigger is the same, the structure and operating environment of actuators are characterized differently, and thus, the advantages and disadvantages also differ. For example, EAH inevitably requires water-containing environments, while IPMC can be used in dry conditions for a few hours or days because it is composed of ionic polymer (i.e., IPMC contains ions itself) and its lifespan can be increased further by encapsulation that can prevent solvent evaporation. In this part, we review materials and structures of DEA, EAH, and IPMC actuators, and highlight different strategies to improve their actuation performance.

2.1.1. DEAs

The working mechanism and structure of a DEAs are presented in **Figure 2**a, and photographs of a DEA before and after actuation

Table 1. Summary table for electrically driven soft actuators in the view of types, advantages, limitations/challenges, and applications.

Types of actuators		Advantages	Limitations/challenges	Applications	Ref.
Electroactive polymer (EAP) actuator	Dielectric elastomer actuator (DEA)	Fast response	High driving voltage	Micromanipulator	[15,57,59,64–73,75–77]
			Short device lifetime due to dielectric breakdown	Underwater soft robots	
		Ease of fabrication	Irreversible dielectric breakdown due to high driving voltage	Biomimetic actuator (lenses)	
				Haptics	
	Electroactive hydrogel (EAH) actuator	Low driving voltage	Limited operation voltage (water electrolysis disruption and perturbation occur over 1.23 V)	Underwater soft robots	[83,88–91,93]
		Can be used in water-containing environment	Low blocking force	Microfluidic valve	
		Lightweight	Limited operating environment (electrolyte environment)		
	Ionic polymer–metal composite (IPMC) actuator	Can be used without electrolyte environment	High material cost	Underwater soft robots	[31,32,94,106,107,157,158,174]
		Can be used in water-containing environment	Poor environmental safety		
		Low driving voltage	Low blocking force	Micromanipulator	
		Fast response			
		Long-range stroke	Short lifetime		
Electrothermal actuator (ETA)	Bilayer ETA	Long-range stroke	Low design diversity	Biomimetic actuator (insects and plants)	[14,24,33,35,36,111,113,114,130,133,136]
		Lightweight			
		Can be designed in thin film form	High driving voltage	Micromanipulator	
	Thermally-triggered shape memory polymer (SMP) actuator	High-design diversity (programability)	Irreversible actuation (require external mechanical force to make reversible actuation)	Microfluidic valve	[4,39,42,125–129,133–135]
		Ease of fabrication		Micromanipulator	

are shown in Figure 2b.[49] The thickness of the dielectric elastomer sandwiched with two compliant electrodes is reduced by electrostatic Maxwell stress when a voltage is applied. Therefore, the working principle of DEAs is based on the planar expansion and axial contraction when the electric field distribution of the dielectric material is changed by the external electric sources, making response of DEAs fast up to a bandwidth of 500 Hz.[3] The generated Maxwell pressure of a dielectric elastomer upon application of the electric field can be calculated from Equation (1)[44]

$$p = \varepsilon_0 \varepsilon_r \left(\frac{V}{z} \right)^2 \tag{1}$$

where p refers to the Maxwell pressure, ε_0 is the vacuum permittivity, ε_r is the permittivity (dielectric constant) of the dielectric material, V is the applied voltage, and z is the thickness of the dielectric elastomer. The dielectric material for DEA should satisfy high dielectric constant and high breakdown stress but they are on the trade-off relationship. Many studies have been conducted to analyze these characteristics of diverse materials, and this is well demonstrated in a review paper with chemistry perspectives.[44] Various materials are being used as dielectric materials, representatively, such as acrylic elastomers

(e.g., VHBs from 3M), natural rubber, polyurethane (PU) elastomers, polar elastomers, and silicone elastomers.[44] For compliant electrodes, they should not interfere with the natural contraction and actuation of the dielectric material and should be robust enough to maintain high electrical conductance for rapid electric charging under high strains. As materials satisfying these conditions, carbon-based materials (carbon powder, grease, and conductive carbon black particles),[50,51] and metallic nanowires[52] have been frequently used for the fabrication of stretchable electrodes, and some literature comprehensively analyzed the flexible electrode.[45]

DEAs have been extensively studied because of their rapid response, large actuation strain, low cost, ease of fabrication. Furthermore, soft dielectric materials possess human-tissue like mechanical properties (e.g., stress–strain relation similar to that of the human muscle) that make them ideal for the applications as artificial muscles, and soft robots.[53] A typical DEA has energy efficiency of 26%, similar to that of human muscle (i.e., 20%)[54] and their blocking force varies from a few mN to 1000 N, depending on the materials and structures.[3,51] The energy density of DEAs is also scale-invariant, below 0.02 kJ kg^{-1},[55] thus they can be used for microrobots and microfluidics in scales ranging from millimeter to micrometer.[56]

**ADVANCED
SCIENCE NEWS**

www.advancedsciencenews.com

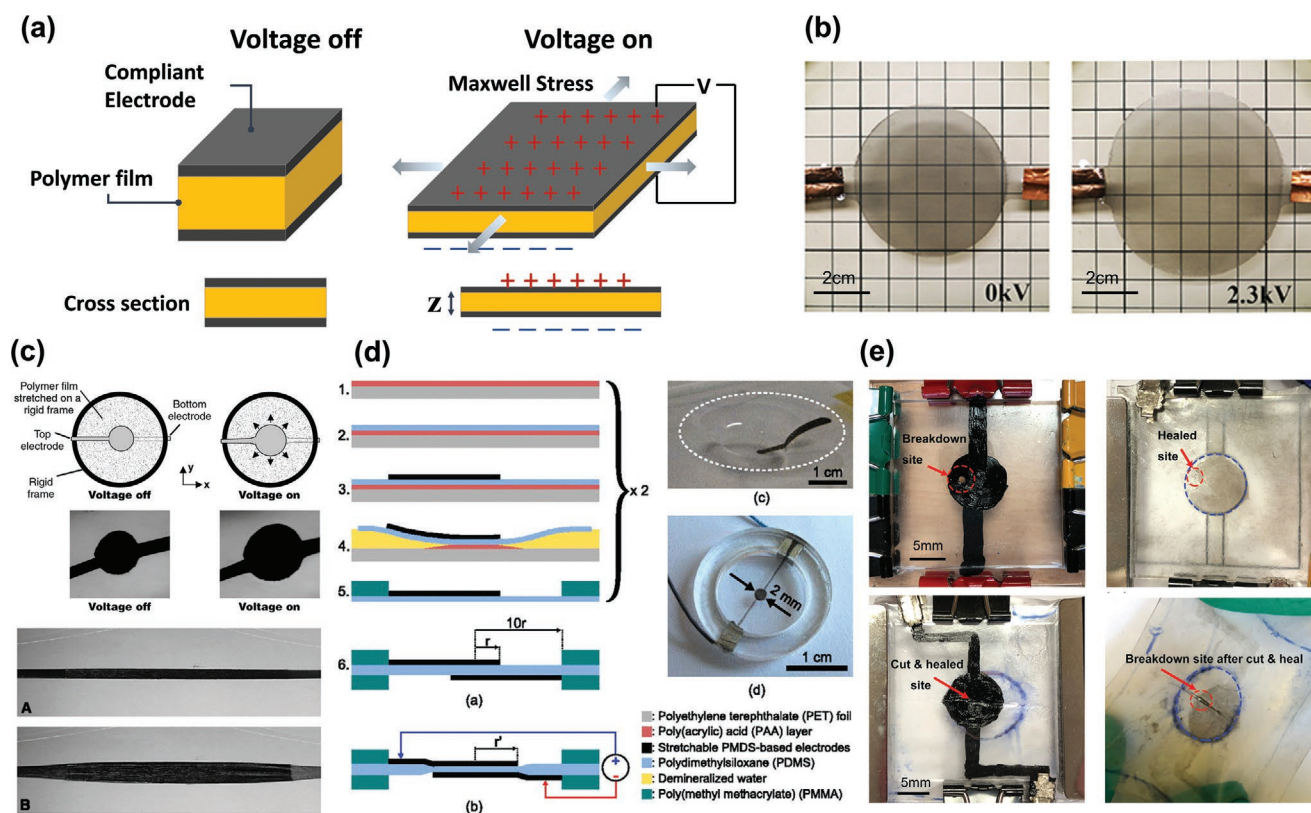**ADVANCED
MATERIALS
TECHNOLOGIES**

www.advmattechnol.de

Figure 2. a) Schematic illustration of the working principle of DEAs. b) Photographs of a DEA actuator under on/off electrical input voltage. Reproduced under the terms of the CC-BY-4.0 license.[49] Copyright 2019, The Authors. Published by Frontiers Media. c) Prestretch of elastomer film by rigid frame for implementation of large strain actuation in a planar direction. Reproduced with permission.[57] Copyright 2000, The American Association for the Advancement of Science. d) Fabrication process of 33 μm thick dielectric elastomer layer by pad-printing method for low driving voltage. Reproduced with permission.[70] Copyright 2015, AIP Publishing. e) Photographs of a self-healable DEA actuator and its self-healing capability after electrical breakdown and mechanical damage. Reproduced with permission.[78] Copyright 2019, Wiley-VCH.

As shown in Figure 2c, Pelrine et al.[57] developed DEA structures with prestretching to enhance the actuation strain range in a planar direction. When the DEA elastomer becomes thinner, the electric field increases resulting in the larger actuation. The prestretching of elastomer improves the property of DEA by a few mechanisms.[58–60] First, prestretch suppresses the electromechanical instability during actuation. Second, the prestretch makes the DEA thinner, which decreases the operating voltage. Third, prestretch can improve the stiffness of the elastomer itself. The elastomer behaves like polymer melt before the prestretch while the polymer backbone is aligned in the prestretched elastomer, which results in stiffness improvement of the elastomer.[61] Consequently, prestretching of a dielectric material can improve the breakdown strength[62] as well as actuation strain.[63] Further explanation is well described in these papers. An elastomer film with a thickness of 10–200 μm was prestretched and fixed by a rigid frame, and as compliant electrodes, conductive carbon greases on both parts of the elastomer planar were stencil-printed to a smaller size than the rigid frame. The planar expansion actuation strain reported to be greater than 117% for silicone elastomer and greater than 215% for the acrylic elastomer. A large actuation strain means that the actuator can have a high energy density of elastic deformation, which is an important factor in the robotics application of DEAs. Since then, it has been widely known that prestretching

dielectric material increases the stability of mechanical actuation. Therefore, this method has been generally used in various DEAs, and it has been demonstrated that controlling the degree of prestretch has a great effect on the performance such as range of actuation strain, response time, etc.[59,64,65] However, the prestretching limits the design flexibility and stretchability due to the rigid frame. In addition, while DEAs show large strain actuation in the planar direction, their strain range in the axial direction is limited. These challenges hinder the design diversity of actuators and restrict their applicability to flexible artificial muscles. In various studies, these issues have been resolved using structural designing such as multistacking[66–69] or designing DEAs with a rolling structure,[51] eliminating the need of a rigid frame for prestretching.

The biggest remaining challenges in the design of high-performance DEAs are their high driving voltage (e.g., a few tens of kilovolts), irreversible dielectric breakdown, and device lifetime. There are efforts to decrease the driving voltage by reducing the thickness of the elastomer.[70–73] For instance, Poulin et al. developed a DEA with 3 μm thick dielectric elastomer layer and compliant electrodes through pad-printing method. The actuator produced a lateral actuation strain of 7.5% under 245 V (Figure 2d).[70] While fabrication of the DEAs with thicknesses less than 20 μm was a grand challenge in this area, the pad-printing method in this study offered a robust

manufacturing strategy to produce DEAs with a thin, stable, and uniform elastomer membrane as well as compliant electrodes. Later, Ji et al.[72] developed a process for transferring carbon nanotubes (CNTs) and poly(alkylthiophene) compliant electrodes onto a prestretched PDMS membrane with the thickness of 1.4 μm using Langmuir–Schaefer technique and achieved 4% strain with an operating voltage of 100 V. As the thickness decreases, the mechanical property of the electrode cannot be ignored during the operation the DEA, while a thick dielectric elastomer is used, mechanical properties (i.e., mechanical constraints) of electrodes can be neglected because the electrode thickness is relatively thin. Therefore, research is being focused on developing ultrathin dielectric elastomers and highly stable and stretchable electrodes.[73]

There have been attempts to prevent device failure that causes breakdown in dielectric elastomer using high permittivity materials.[46,74,75] The widely used methods include a) blending or mixing the high permittivity nanomaterial with elastomer in the form of nanocomposites; b) chemical modification of elastomer with high dipole moment group. For details of novel materials and compositions for increasing the dielectric material permittivity, we recommend the reader to read a comprehensive review reported by Opris.[74]

For reliability and lifetime improvement of DEAs, studies have been conducted to enable self-healing of dielectric materials with dielectric breakdown by designing self-healing materials,[76–80] which refer to substances that repair damages by themselves through recombination of functional groups by externally applied stimuli. Zhang et al. reported a room-temperature self-healing mechanism using metal–ligand interaction.[78] It has been shown that the interaction between the styrene–butadiene–styrene block and the methyl-thioglycolate-modified butadiene block (material called thermoplastic methyl thioglycolate-modified styrene–butadiene–styrene elastomer) can re-establish the bond of the damaged site. As depicted in Figure 2e, the material self-heals well even after there is an electrical breakdown in the form of a pinhole or a mechanical breakdown in the form of a line. Before any damage, the relationship between driving voltage and strain of pristine DEA is around 30 kV mm^{-1}. The damaged and self-healed DEA shows no significant difference in this relationship for either electrical breakdown or mechanical damage. In addition, the dielectric strength after dielectric breakdown and mechanical damage were restored to 67% and 29% of their original stages, respectively.

Through these various researches, state-of-the-art DEA can have a high actuation strain range, high energy density, and lightweight so that it has the potential to be used in various robotic muscles due to its lightweight. Many studies have been conducted to overcome the dielectric breakdown phenomenon caused by the high driving voltage and the limited device lifetime, however a solution that can solve all the problems simultaneously has not yet been developed. Therefore, further research is necessary to solve both problems simultaneously.

2.1.2. EAH Actuators

The driving principle of EAH actuators and their configuration are presented in **Figure 3**a. They are composed of a soft responsive polyelectrolyte with swelling/shrinking and/or bending/unbending features. Upon application of the external electric field through two electrodes in the electrolyte medium, redistribution of the ion charge in the internal polymer structure leads to the osmotic pressure gradient in the polyelectrolyte, causing mechanical shape changes due to asymmetric solvent absorption. The response of EAH is relatively slow (response time of 60 s and bandwidth of 0.05–0.625 Hz) because of the slow movement of ions and the solvent absorption process.[81–83] Various hydrogels are being developed for EAH soft actuators, including agarose,[84] chitosan,[85,86] poly(acrylic acid) (PAAc),[87] and poly(2-acrylamido-2-methylpropane-sulfonic acid) (PAMPS),[88] and more recently self-healing polymers.[81] Compared to other types of responsive hydrogels actuated by various stimuli (heat, light, pH, etc.), EAH soft actuators offer advantages of underwater applicability and remote controllability by an electric field, making them appealing in drug and tissue engineering, underwater soft robotics, cell-based devices, and biomimetic engineering.[89,90] Especially, in the field of biomimetic EAH, there is a comprehensive review paper.[84] In addition, the actuation direction of EAH actuators can be controlled by the type of cations and anions. In a recent paper,[91] three anionic hydrogel acrylamide (AAm)/sodium acrylate (NaCa) copolymers and cationic hydrogel and acrylamide/quaternized dimethylaminoethyl methacrylate (DMAEMA-Q) copolymers have been used to construct walking robots. The bidirectional leg movement of the robot was controlled by designing two different anionic/cationic gels attached to each other, making the robot to move through tuning the direction and frequency of the electric field. However, EAH soft actuators have relatively poor mechanical properties (Young's modulus below 100 kPa),[92] and thus the blocking force is low. Moreover, the electrolyte medium shortens the lifetime of actuators due to disruption and perturbation caused by the water electrolysis, specially under voltages over 1.23 V.

To overcome these drawbacks of EAH soft actuators, various composite materials and structures have been proposed. For example, multifunctional micelles were in situ copolymerized in neutral and cationic monomers to improve the mechanical properties of the hydrogel such as fatigue resistance, strength, and responsiveness to environmental stimuli, as shown in Figure 3b.[93] By the in situ polymerization synthesis of micelles, an actuator with prominent strength, toughness, and Young's modulus of a few hundred kPa was developed. When a voltage was applied to the polyanion gel, the movement of the counterion toward the cathode changed the osmotic pressure gradient, generating a bending deformation for the actuator. Bending angles of about −80° and +60° were achieved when −20 to 20 V were applied to the actuator. In another study, Santaniello et al.[92] prepared hydrogel/cellulose rod-like nanocrystals (CNCs)-based nanocomposites by incorporating CNCs into hydrogels (Figure 3c). Given unique characteristics of CNCs, including piezoelectricity, low density, and mechanical strength, their contribution to the physical cross-linking of the proposed polymeric matrix improved the mechanical characteristics of the hydrogels and led to a subvolt electroresponsive system. (≈5 mV cm^{-1}). Yang et al.[88] reported a nanocomposite electroactive actuator made of poly(2-acrylamido-2-methylpropanesulfonic acid-co-acrylamide) (PAMPS-co-AAm)
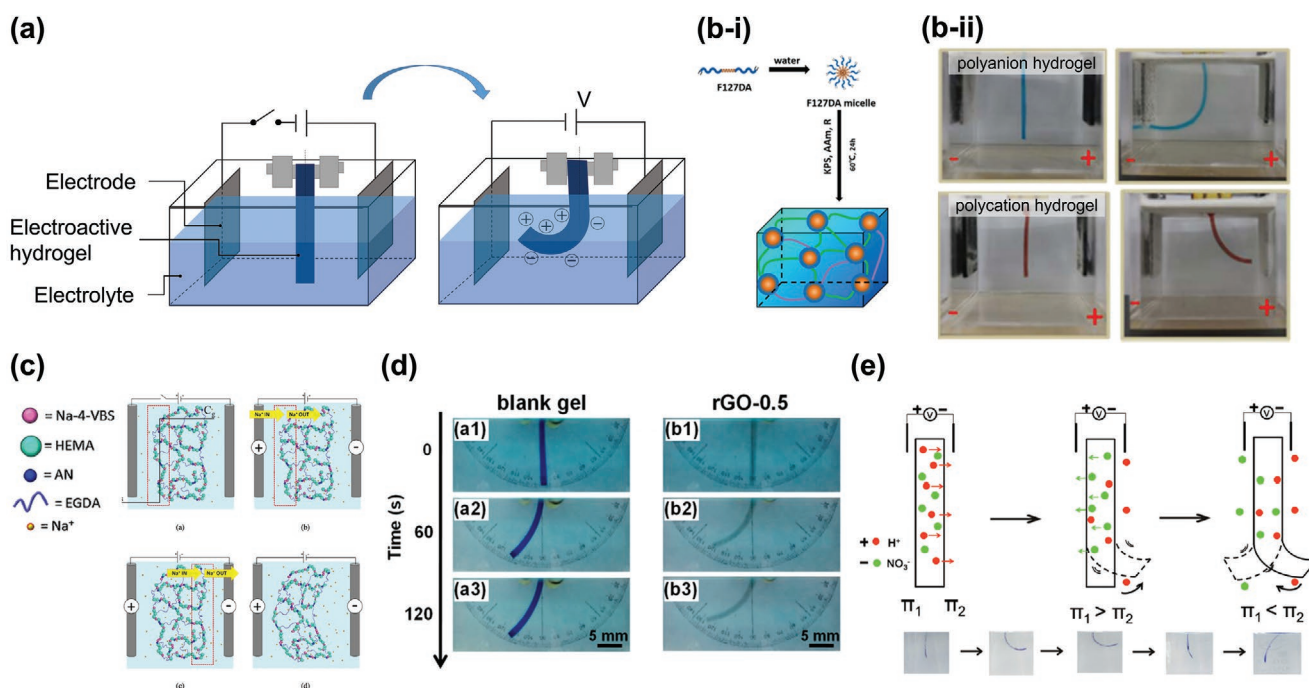
Figure 3. a) Schematic illustration of the working principle of EAH actuators. b) Multifunctional micelles for improving the fatigue resistance, strength, and responsiveness to environmental stimulus. i) Schematic of in situ polymerization using multifunctional micelles and ii) bending behavior of the polyanion and polycation hydrogel under input voltage in the Na_2SO_4 solution. Reproduced with permission.[93] Copyright 2016, American Chemical Society. c) Combination of CNC and polymeric matrix of NA-4-VBS, HEMA, and AN for achieving subvolt electroresponsive system. Reproduced with permission.[92] Copyright 2017, IOP Publishing Ltd. d) Nanocomposite using rGO and PAMPS-co-AAm for improving mechanical properties of the material and actuation performance. Reproduced with permission.[88] Copyright 2017, American Chemical Society. e) Nanocomposite hydrogel (Al-NC gel) for enhancing mechanical properties of hydrogel and enabling bidirectional actuation. Reproduced with permission.[83] Copyright 2019, RSC Pub.

and reduced graphene oxide (rGO) that has a bending response to electrical stimulation (Figure 3d). The combination of the polymer matrix and rGO nanosheets improved the energy dissipation while forming prominent electrical conductivity. This high-performance actuator was used to lift objects in underwater environments.

In another study, Jiang et al.[83] proposed an $Al(OH)_3$ nanoparticles-based nanocomposite hydrogel (Al-NC gel) with enhanced mechanical properties of the hydrogel for EAH actuation. The $Al(OH)_3$ nanoparticles were used as multifunctional crosslinkers to provide good mechanical characteristics with high tensile and compressive strengths of 2 and 35 MPa, respectively. The authors have shown that the bending direction and magnitude of the actuator could be designed by changing the composition of the nanocomposite, as depicted in Figure 3e. Although recent research on EAH actuators has improved their mechanical properties, it is still challenging to enhance the lifetime of materials due to their requirement of the high electrical driving voltage.

Despite these recent efforts to solve the poor mechanical properties and low blocking force of EAH actuators, there is still an unavoidable limitation that an electrolyte environment is required for the operation of EAH. There are three main reasons for the need of an electrolyte environment. First, it is essential to generate an osmatic pressure, which is the main driving force of EAH actuators. Second, electrolyte maintains the gel state for the reliability of hydrogel under repeated mechanical deformations. Third, in order for the ions to move

when the electrical field is generated to EAH actuators, the gel network must be functionalized under a specific electrolyte.[91] Therefore, by the needs for such electrolytes, the lifespan of actuators is limited due to the electrolysis of water occurring above 1.23 V, and it is still challenging to the increase the lifetime of EAH.

2.1.3. IPMC Actuators

To compensate for the limitations of hydrogel actuators (i.e., electrolyte environment and operating voltage), researchers have developed IPMC actuators. In case of IPMC actuators, water-containing ionic polymers are used as a functional layer, and metal composite electrodes are directly attached to both sides of the ionic polymer to provide the electric field and to prevent water drying.[94] The working principle of IPMC actuators is similar to that of hydrogel actuators based on the ion cluster flux and electroosmotic flow of water between two electrodes (i.e., from anode to cathode) under an electric field, as shown in **Figure 4**a,b.[95] Under an electric field, mobile ions (e.g., metal cations) are diffused to the negative electrode, resulting in the asymmetric volume change of IPMC actuators due to the changes of the electrostatic, elastic, and osmotic interaction forces of the ion clusters.[96] Therefore, their response is slow for similar reasons of the EAH actuators but generally a bit faster, because IPMC actuators do not require the solvent absorption process. The response time can be further improved
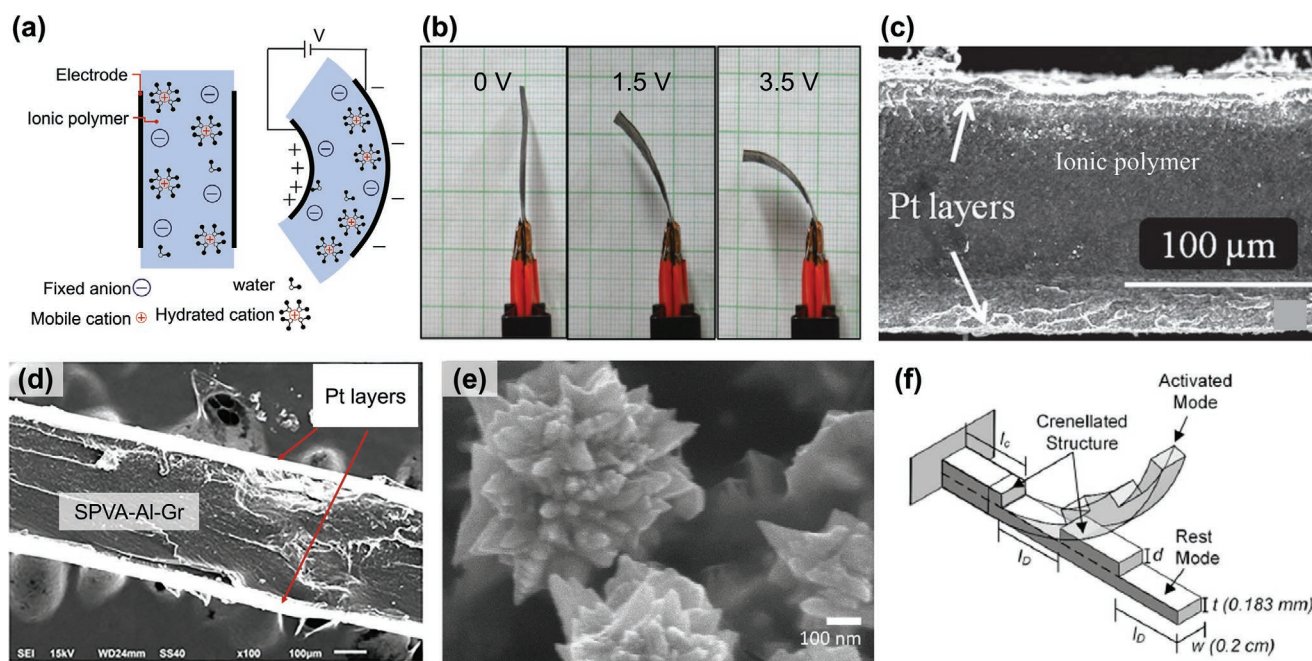
**ADVANCED
SCIENCE NEWS**

www.advancedsciencenews.com

**ADVANCED
MATERIALS
TECHNOLOGIES**

www.advmattechnol.de

Figure 4. a) Schematic illustration of the working principle of IPMC actuators. b) Photographs of the actuation of an IPMC actuator under various input voltages and actuation performance. Reproduced with permission.[95] Copyright 2018, Elsevier Ltd. c) SEM image of the representative structure of IPMC actuators. Reproduced with permission.[97] Copyright 2012, Elsevier Ltd. The bright edges are the Pt electrodes, and the middle dark zone is the ionic polymer. There are diverse strategies to improve the actuation force and speed, such as d) adding various supporting materials including aluminium oxide and graphene to ionic polymers. Reproduced with permission.[95] Copyright 2018, Elsevier Ltd. e) Applying nanothorn-shaped electrodes. Reproduced under the terms of the CC-BY-4.0 license.[105] Copyright 2014, The Authors. Published by Springer Nature. f) Using a crenellated structure to optimize the structure of the IPMC actuator. Reproduced with permission.[23] Copyright 2019, IOP Publishing Ltd.

up to ≈0.38 s by optimized structures and materials.[23] However, unlike hydrogel actuators, the composite structure of ionic polymer and conductive electrode allow the operation of IPMC actuators regardless of the presence of surrounding water and electrolyte. Furthermore, actuators can be used at voltage above 1.23 V, meaning that they have wider working stroke than the hydrogel actuators. To efficiently implement these working mechanism and advantages, typical IPMC actuators are designed with the structure of an ionic polymer layer sandwiched between two conductive electrodes (see Figure 4c).[97] As conductive materials for the electrodes, platinum (Pt) and gold (Au) are widely used because of their electrochemical stability and highly conductive properties. Meanwhile, perfluorinated polymers, such as sulfonated (Nafion), perfluorosulfonic acid (Aciplex), or carboxylated (Felmion) polymer membranes, are generally employed for ionic polymer electrolyte membranes owing to their high proton conductivity and thermochemical stability, and these materials are well reviewed in the literature.[96] Their typical power density is around 2.44 kJ kg^{-1}[98] and the range of blocking force is a few mN[23,95] and the energy efficiency is 2–3%.[99] However, these conventional perfluorinated-based IPMC actuators have some drawbacks, including high material cost, poor environmental safety, low blocking force, and drying during the actuation.

Recently, researches have focused on the development of novel materials to tackle some of these problems. To overcome limitations of perfluorinated ionic polymers in terms of poor environmental safety, various non-perfluorinated materials have been developed. Generally, block copolymer-based actuators,[100]

including sulfonated styrene/methylbutylene diblock copolymer,[101] sulfonated styrene/ethylene/butylene-based triblock copolymer,[102] and Kraton pentablock copolymer,[103,104] are considered as substitutes of perfluorinated actuators due to their low cost, high ionic conductivity, and high mechanical stability. More recently, composite materials have been also developed for IPMC actuators with improved actuation performance. Figure 4d shows a recently reported non-perfluorinated IPMC actuator composed of sulfonated poly(vinyl alcohol), aluminum oxide (Al$_2$O$_3$), graphene, and platinum (SPVA-Al-GR-Pt). In this study, sulfonated poly(vinyl alcohol) was applied as the ionomeric material because of its excellent film forming capacity, designable chemical properties, as well as ion exchange capacity and water retention capacity.[95] In addition, graphene was added to enhance the performance through its superior electrical conductivity, and excellent thermal stability and mechanical properties. Al$_2$O$_3$ was also used to improve the dielectric properties, thermal conductivity, and stability. The resulting SPVA-Al-GR actuator showed superior ion-exchange capacity and water uptake property.

To solve the issues of the low blocking force and actuation range, a number of studies have explored the effects of electric resistance and surface structure of electrodes. The high electric conductivity and large surface area of electrodes can improve the actuation performance by increasing the total transported charges and the accommodation of charges at the interface. For example, platinum nanothorn electrodes exhibited highly improved electromechanical performance compared with the planar Pt electrodes (three- to fivefold increase in actuation

stroke and blocking force), as shown in Figure 4e.[105] The authors explained that these characteristics are related to higher charge transport during actuation. This nanothorn-based IPMC actuator showed improved blocking force (≈20 mN) and actuation range (5 V mm^{-1}) at a low driving voltage (1–3 V).

An alternative way to enhance the blocking force is to improve the stiffness of the ionic polymer. The most widely used approach is to incorporate nanomaterials (i.e., CNTs, graphene, and metallic nanoparticles) into ionic polymers, improving the backbone strength of ionic polymers as well as their electrical conductivity. However, addition of nanomaterials reduces the actuation stroke because a trade-off relationship between stroke and flexibility of actuators. Structural modification and optimization have also been proposed for the performance improvement of IPMC actuators. Figure 4f, for example, shows the application of a crenellated structure of an IPMC actuator which greatly increased the flexibility of the actuator while maintained its mechanical strength.[23]

Overall, research is still being actively conducted to overcome the abovementioned problems and to optimize IPMC actuators through design of materials and structure.[106,107] In addition, the state-of-the-art studies have made great progress toward understanding and improving the IPMCs actuators. Therefore, it is clear that IPMC actuators will be effectively used in various applications, especially for the actuators in a water-containing environment due to their superior actuation performance even in water.

2.2. ETAs

Unlike EAP actuators, ETAs, including bilayer ETAs and SMP actuators, are actuated by the generated heat during Joule heating. They have a disadvantage that actuators inevitably require a conductive layer as heating element. However, ETAs have attracted much attention recently because they are considered as an outstanding alternative to solve the bottleneck problems of electroactive polymer actuators, such as a short-range working stroke and limited working environment (e.g., electrolyte-containing environment for hydrogel actuators), which led to the publication of review papers that are focused on only ETA recently.[108,109]

2.2.1. Bilayer ETAs

The driving mechanism of bilayer ETAs is based on a strain mismatch of two layers at elevated temperatures due to the difference between their CTE values. As shown in **Figure 5**a, bilayer actuators are generally composed of a high CTE layer, a low CTE layer, and a thin conductive film for Joule heating in between them.[110–112] When an electrical current is applied to the heating layer, the high CTE layer and low CTE layer expand due to the generated heat. As the thermal expansion of the low CTE layer is relatively small, actuators bend toward the low CTE layer (Figure 5b).[113] Thus, their response time highly depends on the thickness and specific heat capacity of the high CTE layer (from 42 to 5 s), because the thickness and specific heat capacity are directly related with the time to absorb the thermal energy from the heater.[14,114] Because of the working

mechanism and structures, bilayer ETAs have the advantages of no limitations in the working environment, long working stroke, lightweight, and thin film form. However, to ensure better performance, various design parameters for each layer should be considered. a) High CTE layer: the material used as a high CTE layer should have adequate flexibility to maintain its overall shape even in a suspended state, but it must be able to bend easily under applied heat, as well as have a high CTE. b) Heating layer: the heating materials should have a high electrical conductivity for a low driving voltage and a high thermal conductivity for rapid heat diffusion. In addition, it is necessary to have strong adhesion with both high CTE and low CTE layers to avoid delamination during repeated actuation. c) Low CTE layer: this layer should be made of thin film-type material with low CTE to reduce the bending constraints. d) The entire structure should have strong adhesion between layers for mechanical stability under repeated mechanical deformation. It also should be fabricated as a thin film from lightweight materials for practicality. To develop bilayer ETAs that satisfy these conditions, researchers have utilized polymer nanocomposites[115–118] or a combination of polymer and metal thin film[119] that have already been developed in the field of soft devices[120–126] and high performance electronics.[127–129] Figure 5c shows one of the most representative structures and materials of bilayer ETAs that meets the abovementioned conditions.[24] In this paper, polydimethylsiloxane (PDMS) is used as a high CTE layer, PDMS/SWCNT composite is used as a heating layer, and SWCNT fiber film is used as a low CTE layer. However, despite many studies including structural optimization so far, there are still challenges for achieving programmable shape outputs and low driving voltage.

Design diversity of bilayer ETAs should be developed further. For an actuator to be used in practical application, broad diversity of actuation shapes is required. However, the conventional bilayer ETAs exhibited only a simple motion change caused by one-directional bending. To solve this problem, the direction of thermal expansion was controlled using the anisotropic properties of aligned materials in early research, but this limits the material selectivity and requires high driving voltage. Alternatively, Ahn et al. recently controlled the heat distribution using a heating layer with heterogeneous conductance, thereby improving the design diversity (Figure 5d).[114] Alternatively, Yao et al. reported a programmable actuator by attaching stiff materials to the high CTE layer, as shown in Figure 5e.[113] In addition, there are many novel methods, such as the use of the anisotropic expansion of actuating materials (Figure 5f)[130] or multiresponse materials[131–135] to control the shape output.

The driving voltage of bilayer ETAs should be lowered for applications to portable devices. Generally, CNTs, which can be easily aligned, are selected as a heating material, but this approach has a fundamental limitation that actuators often require a high driving voltage (≈40 V) because of the relatively high electrical resistivity of CNT films.[136] As a result, various composite materials, such as CNT/Ag nanowire composites[114] and graphene oxide/Ag nanoparticle composites[137] as well as highly conductive metal nanowires have recently been used to lower the driving voltage.

It can be seen that many studies have been conducted to address the problems of high driving voltage and the low
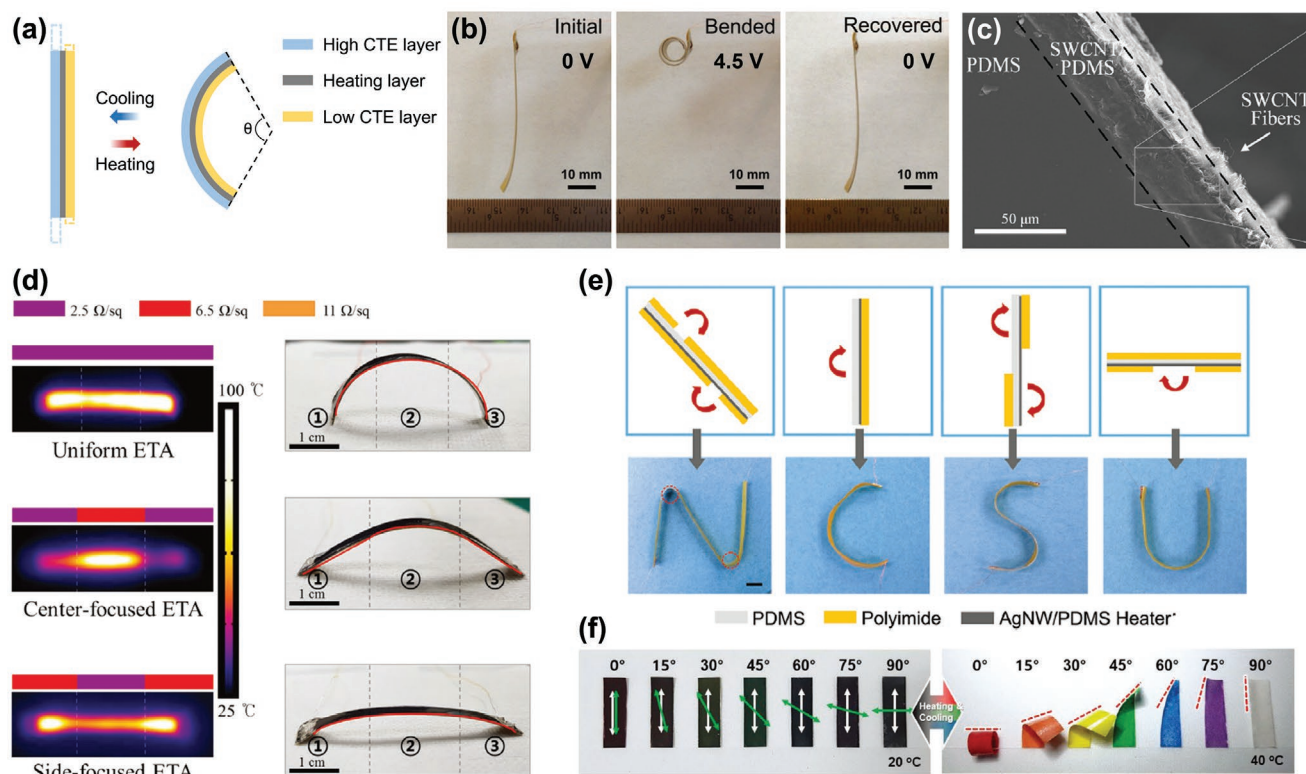
**ADVANCED
SCIENCE NEWS**

www.advancedsciencenews.com

**ADVANCED
MATERIALS
TECHNOLOGIES**

www.advmattechnol.de

Figure 5. a) Schematic illustration of the working principle of bilayer ETAs. b) Photographs of the actuation of a soft actuator under various input voltages. Reproduced with permission.[113] Copyright 2017, RSC Publishing. c) SEM image of the representative structure of bilayer ETAs. Reproduced under the terms of the CC-BY-4.0 license.[24] Copyright 2018, The Authors. Published by Springer Nature. The PDMS layer on the left region has a high CTE, the PDMS/CNT composites on the middle region is the conductive layer, and the CNT fiber on the right region has a low CTE. d) Shape designing by varying the heat distribution of the heterogeneous conductance-based bilayer ETAs. Reproduced with permission.[14] Copyright 2019, Wiley-VCH. e) Combining stiff materials with active layers to achieve programmable actuation. Reproduced with permission.[113] Copyright 2017, RSC Publishing. f) Changing the alignment of an anisotropic material for controlled actuation. Reproduced with permission.[130] Copyright 2018, Wiley-VCH.

diversity of actuation shapes, but a solution that can solve both problems simultaneously has not yet been developed. Therefore, we can conclude that, although bilayer ETAs have a great potential for use in practical applications, follow-up research needs to be conducted to improve the driving voltage and design diversity simultaneously.

2.2.2. Thermally Triggered SMP Actuators

SMPs are functional materials with unique properties that undergo mechanical shape change under chemical,[138] electrical, light,[139] microwave heating,[140] magnetic,[141] and thermal[142] triggers. As shown in **Figure 6**a, when an external force is applied to a thermally triggered SMP at temperatures above its glass transition temperature, the original or permanent shape of the SMP changes to a temporary shape.[40] After that, even if heat and external force are removed, the deformed shape (called as a "programmed shape") of the SMP is maintained. Upon reheating, the stored energy is released, and the SMP automatically recovers its original shape. Their typical power density is around 2.8 kJ kg^{-1},[143,144] and the blocking force ranges from few mN to few hundereds mN,[39,145] and the energy efficiency is around 1–2%.[144] SMPs are widely

used as soft actuators because they can be fabricated in arbitrary shapes, have flexible and deformable characteristics with a short response time (0.11–5 s),[39,145] and their deformed shapes can be programmed. For example, an actuator with a vertical motion can be simply implemented by designing a spring-shaped actuator (Figure 6b).[40] Among SMP actuators, an electrically driven SMP actuator utilizes heat generated by Joule heating for its phase transition, and it is generally composed of thermally triggered SMP (e.g., poly(ε-caprolactone),[50,146] polylactide,[147] and poly(ethylene-co-vinyl acetate),[148]) and composites of conductive nanomaterials (e.g., Ag NPs and graphite sheet)[50,145] that are well reviewed in the literature focusing on SMP composites.[149] For low driving voltage and stable actuation, high electrical conductivity and strong adhesion of electrodes are required. Figure 6c shows an SMP actuator made of carbon fiber felts (CFFs) and epoxy-based SMP composites where conductive networks of the CFFs are established within CFF/SMP composites for Joule heating.[41]

Although SMP actuators exhibit a superior shape changing capacity, low energy consumption, and excellent manufacturability, they suffer from poor actuation reversibility. A conventional one-way SMP actuator can deform from a temporary shape to its original shape only by heating, and an external strain is required to transform it into a temporary shape again.
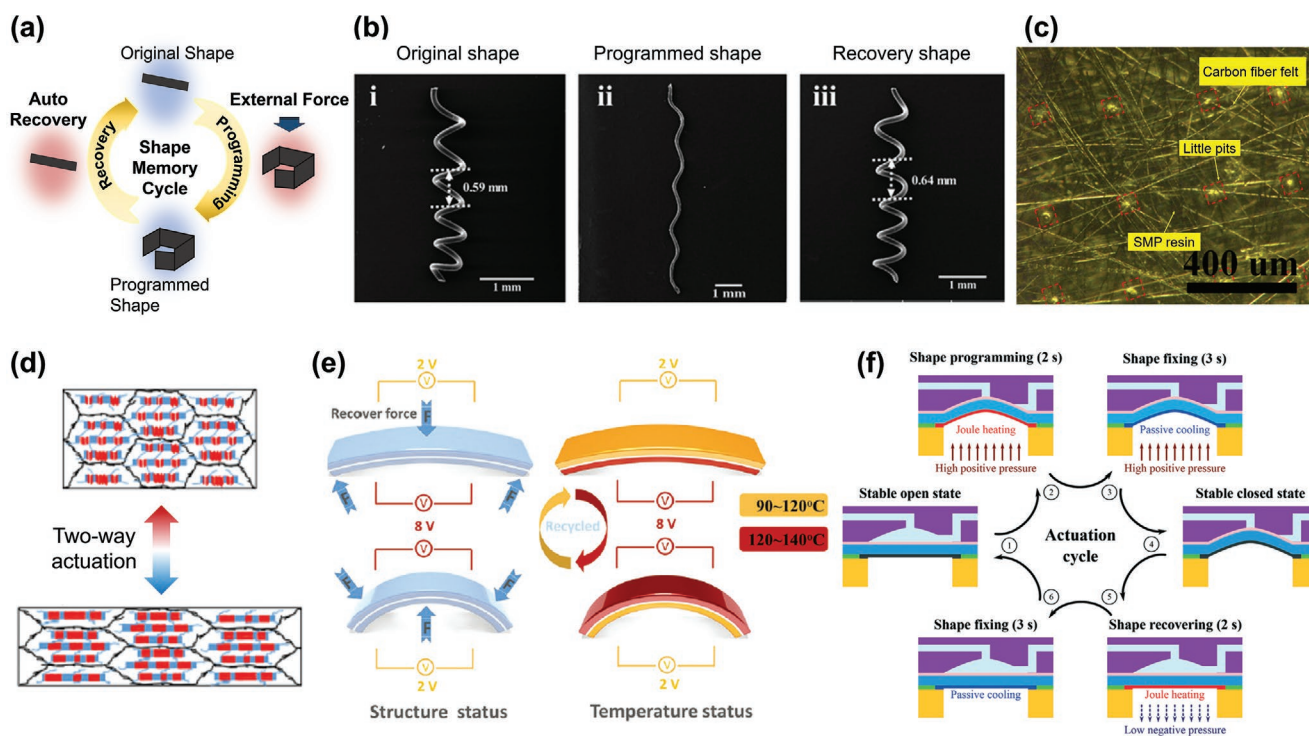
ADVANCED
SCIENCE NEWS
www.advancedsciencenews.com

ADVANCED
MATERIALS
TECHNOLOGIES
www.advmattechnol.de

Figure 6. a) Schematic illustration of the working principle of SMP actuators. Reproduced with permission.[40] Copyright 2018, Elsevier Ltd. b) Photographs of actuation and deactuation shapes of an SMP actuator. Actuation/deactuation shapes can be controlled by external heat and force. Reproduced with permission.[40] Copyright 2018, Elsevier Ltd. c) Optical microscope image of the representative structure of SMP actuators. Reproduced with permission.[4] Copyright 2016, IOP Publishing Ltd. Conductive carbon fibers were mixed with the SMP resin for Joule heating. d) Modification of the chemical structure for a two-way SMP actuator. Reproduced with permission.[39] Copyright 2016, American Chemical Society. e) Using two different SMP actuators simultaneously to enhance the reversibility. Reproduced with permission.[150] Copyright 2016, RSC Publishing. f) Combining SMP actuators with pneumatic actuators. Reproduced with permission.[151] Copyright 2019, RSC Publishing.

This actuation reversibility problem limits SMP actuators from being used in practical applications. Therefore, various studies on chemically engineered SMP materials, bipolymer structures by attaching two SMPs, and multiresponsive materials have been conducted to tackle this problem. The chemically engineered reversible SMPs, which are also called two-way SMPs, are semicrystalline polymers which has a broad range of melting temperatures, as shown in Figure 6d.[39] In addition to the phase transition of one-way SMP actuators, cooling-induced elongation by crystallization and heating-induced contraction by the entropy-driven recoiling of oriented chains enable the reversible actuation of semicrystalline SMP. However, this reversible motion comes from simple thermal elongation and contraction; thus, it causes the problem of short-range working stroke. Alternatively, actuators with an SMP bipolymer structure have been developed to promote the reversible motion (Figure 6e). Here, two actuators are physically bonded, and then different electric inputs are applied to each actuator.[150] The temporary shape of one actuator is formed by the force generated when the other actuator is deformed from the temporary shape to the permanent shape. Figure 6f shows another way to implement reversible actuation by combining pneumatic actuators and SMP actuators.[151] The actuation system was developed that can easily control the shapes of SMP actuators through the application of proper force to create a temporary shape using the pneumatic actuator and applying heat using Joule heating.

However, because the aforementioned solutions limit the general advantages of SMP actuators that can be manufactured in arbitrary shapes, there are still many challenges to be solved for completely reversible actuation. Further development of completely reversible SMP actuators will have a significant impact on the field of soft actuators because of the high demand for SMP actuators.

3. Applications

Electrically driven actuators can be used in diverse applications ranging from soft gripper to biomimetic device, microfluidic valve, rehabilitation device, and haptic device. In the following sections, we discuss some of the key applications of electrically activated soft actuators.

3.1. Soft Gripper and Manipulator

This section briefly summarizes the use of EAP actuators and ETAs as a micromanipulator. Compared to conventional manipulators made of rigid components, soft actuators offer high flexibility and softness, making them appealing for various tasks in diverse applications such as gripper for the soft objects and haptic devices. In particular, many applications require soft
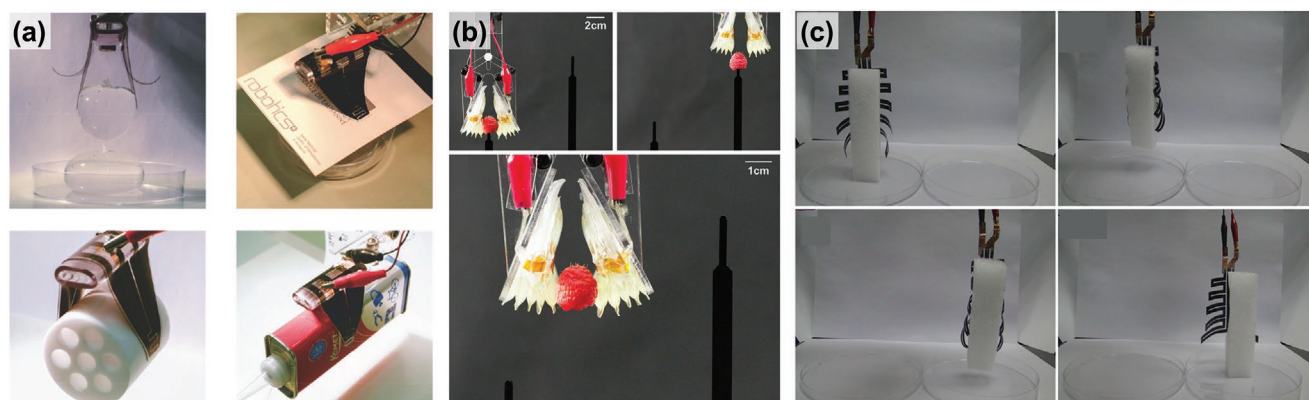
Figure 7. Manipulator application of electrically driven soft actuators. a) Electrically active DEA application on gripper in combination with electroadhesive phenomenon at the gripper tip. Reproduced with permission.[152] Copyright 2015, Wiley-VCH. b) HASEL DEA application on soft robotic gripper for moving raspberry. Reproduced with permission.[76] Copyright 2018, The American Association for the Advancement of Science. c) Bilayer ETA-based gripper with diverse design shapes, like T-shape in the figure. Reproduced with permission.[136] Copyright 2018, IOP Publishing Ltd.

grippers for handling fragile objects, such as eggs and tomatoes. These applications can be classified into two groups based on the purpose of actuators. 1) When strong gripping force and fast response are required with the target shapes fixed, DEA is appropriate because of its merits as discussed in Table S1 of the Supporting Information.[152] 2) When the shapes are random or frequently changed but strong gripping force is not required and they have high thermal stability, bilayer ETA is appropriate because of their high design diversity and compatibility with complex shapes.[136]

Shintake et al.[152] designed a soft gripper robot using DEAs. The gripper was controlled by a circuit that can generate electroadhesive force due to the voltage applied to the electrodes at both ends of the gripper, tuning the gripping force (**Figure 7**a). It was demonstrated that the gripper robot could pick up fragile eggs, balloons, and even flat paper that was difficult to grip with conventional grippers. Among DEAs, hydraulically amplified self-healing electrostatic (HASEL) DEA has the advantage of making a large strain change owing to the motion of liquid surrounded by the dielectric shell, and therefore it can be used as a gripper.[76,153] Stacking of this donut-shaped structure makes much larger deformation by electric actuation. It has been shown that fragile objects, such as raspberries and raw eggs can be transported due to the high softness and controllability of the actuator (Figure 7b).[76] In recent days, EAHs were also utilized as a millirobot gripper whose movement was controlled by both electric and magnetic fields.[154]

As discussed earlier, although bilayer ETA-based manipulators have the disadvantage of low gripping force owing to their driving principle, they can be designed with diverse shapes such as hand-shape, T-shape, and X-shape.[136] For example, Li et al. prepared an highly oriented CNT paper, so they could fabricate multiform actuations with diverse electrode designs. Using this design diversity, they fabricated a distinct stack-T-shaped manipulator that could work like the legs of an insect or as robot manipulators. This manipulator could lift up a polystyrene foam pillar (1.2 g) and move it to another place (Figure 7c). Like this application, the bilayer ETAs show much more design diversity than EAP actuators. Therefore, it is expected

that bilayer ETA-based manipulators can be effectively used in vacuum or space environments because they require design diversity, not a strong actuation force.

3.2. Biomimetic Actuator

Nature always exhibits unique properties, which often give rise to discoveries beyond current human knowledge. In particular, it is important to be interested in living creatures' behaviors, as their movements provide endless inspiration for the design of soft actuators. The development of these biomimetic actuators is not only an academically interesting topic but is also closely related to the commercialization of soft actuators. Therefore, the representative types of electrically driven biomimetic actuators, inspired by insects, marine animals, birds, plants, and human eyes, is discussed below.

Figure 8a shows one of the most representative insect-mimicking actuators.[130,155] Some butterflies have unique color changing characteristics during fluttering motion. In this paper, the authors successfully imitated the motion and color change of butterflies using bilayer ETAs with thermoresponsive color changing materials. When an electric input was applied to the actuator, the wings were fluttered by thermal expansion mismatch, followed by a color change at the edge of the wings. Another example is a worm-like actuator that imitates crawling motions. These crawling actuators, also called as self-walkers, have been actively developed because they are well suited for cargo transfer robots and autonomous robots.[156]

The motions of marine animals with excellent swimming capabilities are valuable design sources for autonomous underwater vehicles (AUVs). Since AUVs have attracted much attention because of the increasing demand for military and commercial applications, imitation of marine animals, including jellyfish,[157] manta ray,[158] fish,[82] starfish,[29] and alligator[159] have been studied. For imitation of these marine animals, hydrogel-based actuators and IPMC actuators are well suited because they can be driven in water-containing environments without performance degradation. Figure 8b shows manta
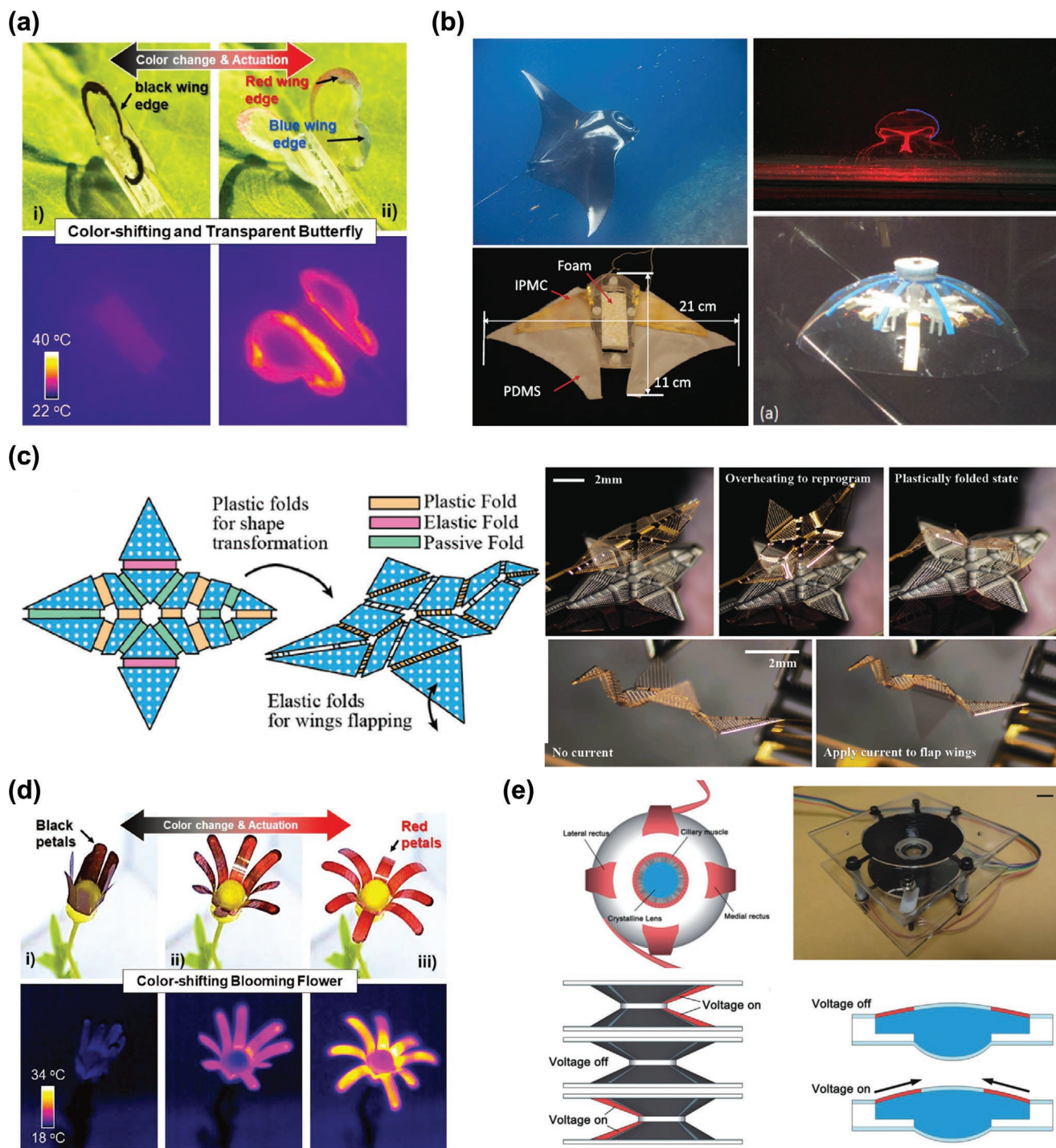
Figure 8. Biomimetic applications of the electrically driven soft actuators. Electrically driven soft actuators can be applied to the biomimetic imitation of a) the color changing characteristic of butterflies. Reproduced with permission.[130] Copyright 2018, Wiley-VCH. b) the flapping motion of manta ray and jellyfish. Reproduced with permission.[157,158] Copyright 2012, Taylor and Francis Group, LLC and Copyright 2012, IOP Publishing Ltd. c) Wing's flapping motion of birds. Reproduced with permission.[11] Copyright 2020, Wiley-VCH. d) The color changing and inhomogeneous swelling/shrinking characteristics of plants. Reproduced with permission.[130] Copyright 2018, Wiley-VCH. e) The motion of human eyes for controlling the focal length. Reproduced with permission.[161] Copyright 2019, Wiley-VCH.

ray- and jellyfish-inspired IPMC actuators. These actuators exhibited excellent swimming capability with highly efficient thrust by mimicking the actuation mechanism of the marine

animals. A manta ray-inspired robot was fabricated to demonstrate excellent swimming capabilities of manta ray, which comes from a large-amplitude flapping motion of its pectoral

ADVANCED
SCIENCE NEWS
www.advancedsciencenews.com

ADVANCED
MATERIALS
TECHNOLOGIES
www.advmattechnol.de

fins using an IPMC muscle and a PDMS membrane.[158] A jelly-fish-inspired robot mimicked the propulsion mechanism of the real-jellyfish, which is the contraction and relaxation of the bell profile. In this bell shape robot, IPMC was attached on the position of the bell margin and used to actuate periodically for propulsion movement.

The bird wing's flapping motion can also be imitated using ETA. Although the response of the bilayer ETA itself is relatively slow, a structural design allows bilayer ETA to move fast. The fabrication of bilayer ETA through this structural design overcomes the intrinsic limitations of bilayer ETA and enables it to be applied to more diverse applications. For example, Figure 8c shows the crane-inspired bilayer ETA and its flapping motion of wings. By applying the bilayer ETA only on the joint part, fast angle change (up to $10\,000° \text{ s}^{-1}$) of the wings was implemented.[111] The actuators that mimic the wings can be effectively used for small soft flying robots, etc.

The motions of plants are also endless sources of inspiration because they have unique color changing and inhomogeneous swelling/shrinking characteristics. In the case of water absorption/desorption motions, hydrogel and IPMC actuators have been widely applied to imitate these properties due to their superior water absorption abilities. On the other hand, for color changing, bilayer ETAs and SMP actuators have been effectively used. Their temperature change caused by Joule heating facilitates the applications of thermochromic inks, as shown in Figure 8d.[130]

Biomimetic soft lenses are additional applications of the soft actuator.[26,160] They can change their motions and focal lengths like human eyes actuated by dielectric elastomer (DE) film. An annular shape DEA could contract with the voltage, leading to a decrease in curvature; thus, the focal of length could be controlled in a manner similar to the real human eye (Figure 8e). Using the biomimetic soft lens, a human–machine interface could be achieved by controlling the lens using electrooculographic signal.[161] There have been some studies on making soft lens using DEAs. A research group[162] shows the ultrafast tunable silicone lenses which shows 175 µs settling time for 20% focal length change. A tunable Fresnel lens are also developed by using DEA, which change the focal length according to the DEA contraction which result in radius change of Fresnel zone.[163]

In summary, the appropriate types of electrically driven actuators were selected depending on the target motion and usage environments to effectively imitate nature's movements. In the case of imitation of insects, flowers, and wings, bilayer ETAs were used, because the authors tried to imitate the complex motions and color-changing properties, not the strong lift. EAH actuators were used for imitating the flapping motion of marine animals, because they can be actuated in water-containing environments. DEAs were selected to imitate the motion of controlling the focal length of human eyes, because controlling focal length requires precise motion control with fast response. The essence of the biomimetic actuators is not simply to exert a strong force or fast motion, but to accurately take advantage of nature's movements. Therefore, most of the electrically-driven soft actuators with precise movement controllability and design diversity can be effectively applied to biomimetic actuators.

3.3. Microfluidic Valve

Another application of electrically driven actuators is the valves and multiplexing in microfluidic chips. Conventional microfluidic devices have been produced through photolithography in the form of integrated components. However, most valve components based on the MEMS process work by the pneumatic mechanism, which involves the continuous operation of a pump and compressor system. Additionally, the rigid valve system has a potential to damage the elastomer-based microfluidic system as well as a restriction of integration within the microfluidic systems. Accordingly, there have been studies to compensate for the disadvantage of the pneumatic method by reproducing the valve components using an electrically driven actuator, such as SMP and EAH. **Figure 9**a shows an individually addressable, latchable, and reversible microfluidic valve array based on SMP actuators.[151] When only a pneumatic actuator is used as a microfluidic valve, a complex and continuous air pressure system is required for the latchable and individually addressable motions. However, in this study, the unique latchable motion of each valve was realized by combining a Joule heating-based SMP actuator and a pneumatic actuator. As discussed above, the SMP material exhibits a 100-fold change of Young's modulus between a glassy ("hard") state (<40 °C) and a rubbery ("soft") state (>70 °C). Accordingly, the valve could be controlled only under the "soft" condition, but negligible motion was obtained for the valves in the "hard" condition. Therefore, by integrating one heater per valve, it was possible to achieve selective valve control with the application of external pneumatic pressure, which means the only electrical power is needed to change the valve states, while individual air pressure control is not required.

As shown in Figure 9b, a millimeter-size underwater valve was fabricated using a CNC-based hydrogel.[92] The valve was immersed in NaCl solution and fixed to an acrylonitrile butadiene styrene (ABS) frame, and when an electrical stimulus was applied to the electrode, the cantilever constituting the valve was bent to control the opening and closing. Thus, it was shown that this actuator can be used for bioinspired underwater soft robots, and cell-based devices without complex air pressure systems inevitably required in the pneumatic actuators.

In a paper by Kwon et al.,[89] the hydrogel actuator was integrated into a microfluidic chip and used in the size sorting system of embryoid bodies (figure 9c). Size sorting can be used to analyze the reproducibility of ES cells. In this work, when a stimulus was applied to the silver electrodes on both sides of the microfluidic channel, the hydrogel valve was bent accordingly to successfully implement a non-bubble made actuation valve.

3.4. Rehabilitation Device

Conventional rehabilitation devices have been developed using rigid components which made the devices hard to be worn by patients. Recently, soft actuator-based rehabilitation devices have been spotlighted due to their compliance for high degrees of freedom movements. Most of soft actuator based rehabilitation devices are fabricated as pneumatic type due to its safety features and compliance.[164] However, the controllers for the
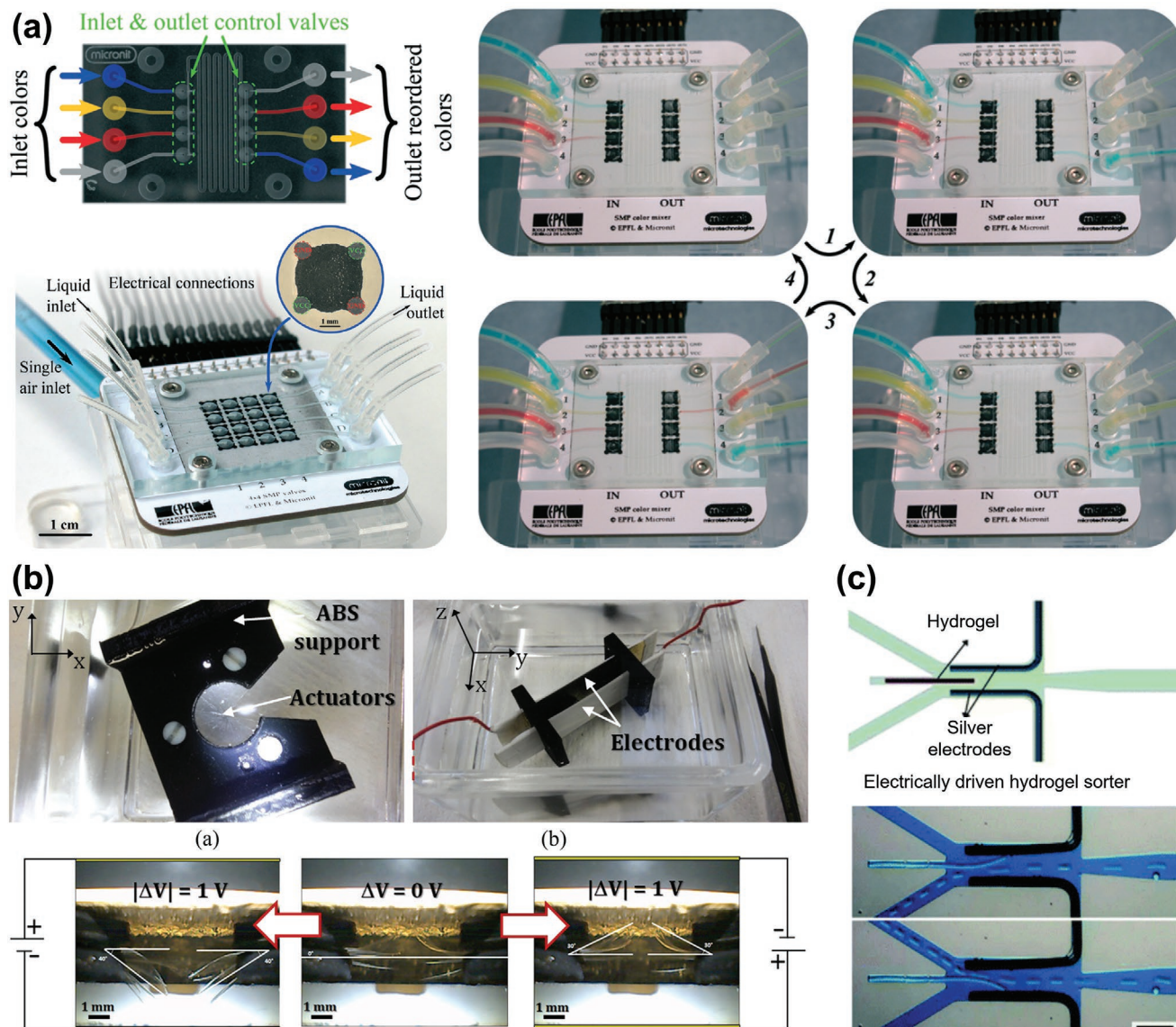
Figure 9. Microfluidic valve application of the electrically driven soft actuator. a) SMP-based latching and multiplexer. Reproduced with permission.[151] Copyright 2019, RSC Publishing. b) CNC/hydrogel actuator-based millimeter-size underwater valve. Reproduced with permission.[92] Copyright 2017, IOP Publishing Ltd. c) Hydrogel actuator integrated microfluidic device for sorting embryo bodies. Reproduced with permission.[89] Copyright 2010, RSC Pub.

pneumatic soft actuators are relatively bulky compared to those for other types. Therefore, other rehabilitation device types have been developed.[165] Among them, electrically driven actuator is suitable for rehabilitation devices due to lightweight, high stretchability, and high compliance.[166] As shown **Figure 10**a, a rehabilitation device for hip joint was fabricated using a plasticized polyvinyl chloride gel and meshed electrode-based DEA.[167] This device could support the hip joint to move the thigh forward and backward. A multilayer structure was applied to achieve the maximum output force of 94 N with a driving voltage of 400 V. Furthermore, the fabricated device could withstand high deformation (>10%) and high stress (>90 kPa), and have variable stiffness. As shown in Figure 10b, a rehabilitation device for a human arm was also developed.[168] Strain-stiffening elastomers

and carbon nanotube electrodes based muscles were utilized to obtain high forces and displacements. The fabricated device showed a peak energy density of 19.8 J kg^{-1} while the displacement corresponded to 24% strain that is similar to the natural muscle. The device could expand linearly at a frequency range between 0.1 and 200 Hz. Regarding the stability of the device, the device could endure over 100 000 cycles of continuous testing without measurable degradation. Figure 10c shows the rehabilitation device for an elbow joint.[169] A 3 × 5 array of stacked DEAs was fabricated to actuate the elbow joint. By stacking and arraying the DEAs, maximum isometric force was measured as 30.47 N. Regarding the range of motion and angular velocity, the rehabilitation device could bend up to an angle of 19.5° and angular velocity of 16.2° s^{-1} under a tensile load of 1 N.
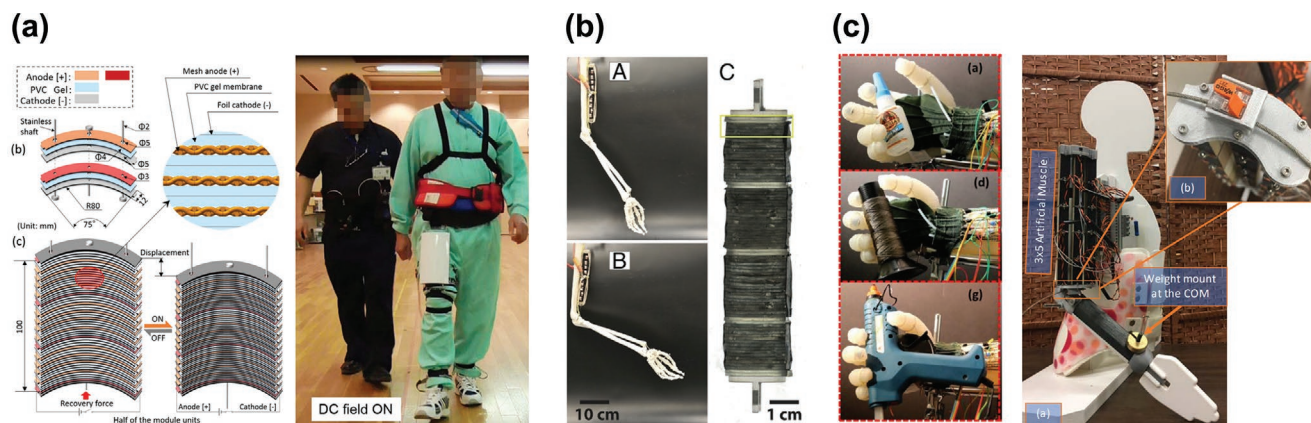
Figure 10. Rehabilitation devices using electrically driven soft actuators. a) Rehabilitation device for hip joint using plasticized polyvinyl chloride (PVC) gel and meshed electrode-based DEA. Reproduced with permission.[167] Copyright 2017, IOP Publishing Ltd. b) Rehabilitation device for a human arm using strain-stiffening elastomers and carbon nanotube electrodes based muscles. Reproduced under the terms of the CC-BY license.[168] Copyright 2019, The Authors. Published by National Academy of Sciences c) Rehabilitation device for elbow joints using staking and arraying the DEAs. Reproduced under the terms of the CC-BY-4.0 license.[169] Copyright 2020, The Authors. Published by IEEE.

3.5. Haptic Device

Soft actuator based haptic devices have been developed for robotic surgery, virtual reality, and augmented reality systems. Haptic devices can deliver human actions to the virtual space and reconstruct haptic feedback sensations from the virtual space. Recently, electrically driven soft actuator based haptic feedback devices have been developed. Amongst electrically driven soft actuators, EAP are suitable to apply for haptic feedback devices compared to ETA owing to their facile fabrication, fast response, high output force, and simplistic design.[170] As shown in **Figure 11**a, a haptic device was fabricated using conductive hydrogel, silver nanowires, and conductive polymers with acrylic elastomer as the dielectric layer.[171] This haptic device showed a maximum force of 43 mN while frequency of

20 Hz was applied and the maximum height of 155 µm with a transformation time of less than a second while electric field of 21.4 V µm^{-1} was applied. Figure 11b shows a multimode haptic device using fluid-filled cavity.[172] When a voltage is applied, the bump is raised because the fluid inside the bump is rapidly forced into the stretchable part. The device has a small size (6 mm × 6 mm × 0.8 mm) and small mass (90 mg). Regarding the performance, the device could generate forces up to 300 mN and deform up to out-of-plane displacements of 500 µm, lateral motion of 760 µm, and response time of 5 ms. Furthermore, human subjects could distinguish normal and tangential movement with up to 80% accuracy. Figure 11c shows digitally controllable tactile bump array driven by IPMC actuators for a refreshable braille display application.[173] The array of soft bump elements was used as the contact interface between the
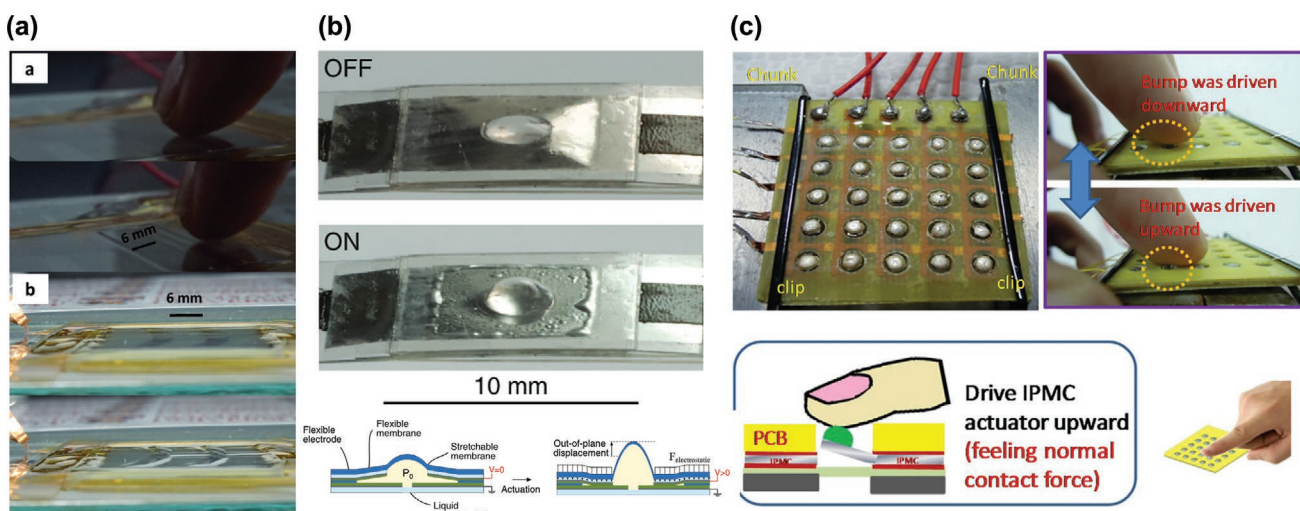

Figure 11. Haptic device using electrically driven soft actuator. a) Haptic device composed of conductive hydrogel, silver nanowires, and conductive polymers with acrylic elastomer as the dielectric layer. Reproduced with permission.[171] Copyright 2017, Wiley-VCH. b) Multimode haptic device using the bump with fluid-filled cavity. Reproduced with permission.[172] Copyright 2020, Wiley-VCH. c) Haptic device using tactile bump array driven by IPMC actuators. Reproduced with permission.[173] Copyright 2018, Elsevier Ltd.

**ADVANCED
SCIENCE NEWS**

www.advancedsciencenews.com

**ADVANCED
MATERIALS
TECHNOLOGIES**

www.advmattechnol.de

fingertips and IPMC actuators, in front of the IPMC-based cantilever beams. The haptic device showed a maximum moment of 1.6 µN m while 8 V square wave of voltage was applied and the maximum forces of 0.68 and 0.55 mN at the bump surfaces for the bump masses of 4.1 and 15.5 mg, respectively.

4. Existing Challenges and Perspectives

Overall, many researches are being actively conducted to develop various electrically driven soft actuators and to utilize them in interesting applications such as soft robotics, biomimetic actuator, microfluidic valves, rehabilitation devices, and haptic devices. However, as mentioned above, there are still many challenges to be solved for the practical use of EAP actuators and ETAs, and many researchers are struggling to solve them. Even though a lot of research solved some parts of the limitations or demonstrated superior performance at a specific point such as driving voltage or blocking force, they could not achieve all the goals simultaneously, as shown in **Tables 1** and **2**. a) DEA actuators: the problems of high driving voltage, irreversible dielectric breakdown phenomenon, and short lifetime need to be solved. Because the latter two problems are mainly caused by the high driving voltage, either developing a novel dielectric elastomer that can be driven at a low driving voltage (<100 V) or fabricating a very thin DEA with a nanoscale thickness can be a

promising solution. b) EAH actuators: they have disadvantages of the limited operation voltage, low blocking force, and limited operating environment. These are inevitable limitations caused by their working principle and following operating environment (i.e., water electrolysis disruption and perturbation occur at the input voltage over 1.23 V). Therefore, instead of solving these problems technically, suggesting an optimal application that does not need to consider these problems (e.g., low blocking force and limited operating environment) such as mimicking the marine animals for the AUVs can be a way to develop the field of EAH actuator. c) IPMC actuators: they have limitations of high materials cost, poor environmental safety, short lifetime, and low blocking force. The problems of IPMC actuators are mainly related to material properties except blocking force. Therefore, further research needs to be focused on the development of a novel ionic polymer with low cost, excellent environmental safety, long lifetime, and high blocking force.[174] d) Bilayer ETAs: the limitations of bilayer ETAs are high driving voltage, low blocking force, and low design diversity. Among them, the current works are more focusing on the increment of the design diversity because a shape-morphing property is becoming key performance index in terms of their applications. To increase the design diversity of bilayer ETAs, it is necessary to develop a more systematic design process and corresponding fabrication method, whereas most of previous studies were conducted with the uncontrollable fabrication process such as

Table 2. Detailed specification for the recently published or the representative electrically driven soft actuators (*Estimated from graph; **Estimated from picture).

Types of actuators		Bandwidth [Hz]/response time [s]	Driving voltage [V]	Blocking force [mN]	Maximum strain [%]	Displacement scale [mm]	Size scale [mm]	Ref.	Power density	Energy efficiency
Electroactive polymer (EAP) actuator	Dielectric elastomer actuator (DEA)	500 Hz	450	9	25	≈3**	10**	[3]	0.02 kJ kg⁻¹[55]	≈26%[54]
		N/A	3800	N.A.	150	67.5	30**	[175]		
		200 Hz	1000	≈1000 N	10	1	10	[51]		
	Electroactive hydrogel (EAH) actuator	60 s	<10	N.A.	Bending-driven flexible actuator	≈44**	15	[82]	–	–
		0.625 Hz*	6–15	N.A.		≈36**	30	[83]		
		0.018–0.05 Hz	100	N.A.		≈80*	60	[81]		
	Ionic polymer–metal composite (IPMC) actuator	N.A.	≈3.5	0.86		≈19	≈25**	[95]	2.44 kJ m⁻³[98]	2.5–3%[99]
		N.A.	≈2.5	N.A.		≈14*	≈40**	[106]		
		≈0.38 s*	≈2	2.5*		≈23*	20	[23]		
Electrothermal actuator (ETA)	Bilayer ETA	42 s	≈25	300		≈100**	≈100**	[114]	–	–
		5 s*	≈30	110 times of weights		≈50**	≈50**	[14]		
		1–200 Hz	≈3	N.A.		≈2**	≈10**	[111]		
	Thermally triggered shape memory polymer (SMP) actuator	5 s*	≈36	677*		≈5**	≈30**	[39]	2.8 kJ kg⁻¹[143,144]	1–2%[144]
		≈1 s*	≈19.5	N.A.		≈0.2	≈3	[151]		
		≈0.11 s	≈2	0.118*		≈30**	≈50**	[145]		

**ADVANCED
SCIENCE NEWS**

www.advancedsciencenews.com

**ADVANCED
MATERIALS
TECHNOLOGIES**

www.advmattechnol.de

spray coating[114] and inkjet printing.[132] e) SMP actuators: the SMP actuators have limitation of irreversible actuation which means they require external mechanical force to make reversible actuation. Many solutions to solve this problem have been reported but they limit the general advantages of SMP actuators such as the manufactural design diversity because of the limited materials and structures. Therefore, further development of completely reversible SMP actuators without limiting other advantages will have a significant impact. In conclusion, research in these areas is still being actively conducted to overcome the abovementioned limitations of electrically driven actuators.[175] Therefore, further study based on the understanding of actuator characteristics will play a vital role in the development of high-demand soft actuators.

5. Conclusion

We reviewed the latest research on electrically driven soft actuators based on their working principles. These electrically driven soft actuators can be driven by an electricity, which is considered one of the most easily accessible types of power sources. Moreover, they can be fabricated in a thin film form with lightweight, which is suitable for practical soft robotics applications, rehabilitation devices, and haptic devices. More specifically, these actuators are classified as EAP-based actuators utilizing the direct response of EAPs under electric input stimuli and ETAs actuators using Joule heating. EAP-based actuators, including DEAs, EAH actuators, and IPMC actuators, are easy to fabricate, and can be used in water-containing environments. Therefore, they are suitable for applications such as marine animal-mimicking soft robots, microfluidic valves, and manipulators. ETAs, including bilayer ETAs and SMP actuators, are suitable for robotic manipulators and biomimetic actuators because of their relatively high design diversity and excellent stability.

Consequently, many previous studies that have been conducted to solve the technical issues of electrically driven soft actuators were reviewed in this article. For example, various nanomaterials (e.g., RGO and CNCs) were added to hydrogels to enhance the actuation force of EAH actuators, and electrode and structure optimizations were performed to improve the actuation performance of IPMC actuators. Also, further studies that combined pneumatic actuators and SMPs or used multiresponsive materials to improve actuators, have been introduced. In conclusion, it can be seen that the research on electrically driven actuators has made great progress, and promising materials and structures to improve the properties of actuators are much better understood. Therefore, we expect that the present study will provide overall research directions in the field of the electrically driven soft actuators and can be viewed as a guideline for the follow-up research.

[1] L. Hines, K. Petersen, G. Z. Lum, M. Sitti, *Adv. Mater.* **2017**, *29*, 1603483.

[2] H. Zhao, A. M. Hussain, A. Israr, D. M. Vogt, M. Duduta, D. R. Clarke, R. J. Wood, *Soft Rob.* **2020**, *7*, 451.

[3] X. Ji, X. Liu, V. Cacucciolo, Y. Civet, A. El Haitami, S. Cantin, Y. Perriard, H. Shea, *Adv. Funct. Mater.* **2021**, *31*, 2006639.

[4] H. Kim, S. kyun Ahn, D. M. Mackie, J. Kwon, S. H. Kim, C. Choi, Y. H. Moon, H. B. Lee, S. H. Ko, *Mater. Today* **2020**, *41*, 243.

[5] L. Belding, B. Baytekin, H. T. Baytekin, P. Rothemund, M. S. Verma, A. Nemiroski, D. Sameoto, B. A. Grzybowski, G. M. Whitesides, *Adv. Mater.* **2018**, *30*, 1704446.

[6] M. T. Tolley, R. F. Shepherd, B. Mosadegh, K. C. Galloway, M. Wehner, M. Karpelson, R. J. Wood, G. M. Whitesides, *Soft Rob.* **2014**, *1*, 213.

[7] H. Jeong, J. Kim, in *International Conference on Robotics and Automation (ICRA)*, IEEE Montreal, QC, Canada **2019**, pp. 7389–7394.

[8] J. Hu, X. Li, Y. Ni, S. Ma, H. Yu, *J. Mater. Chem. C* **2018**, *6*, 10815.

[9] S. Banisadr, J. Chen, *Sci. Rep.* **2017**, *7*, 17521.

[10] H. Lee, C. Xia, N. X. Fang, *Soft Matter* **2010**, *6*, 4342.

[11] R. Fuhrer, E. K. Athanassiou, N. A. Luechinger, W. J. Stark, *Small* **2009**, *5*, 383.

[12] X. Zhao, S. A. Chester, H. Yuk, R. Zhao, Y. Kim, *Nature* **2018**, *558*, 274.

[13] Y. Cao, J. Dong, *Procedia Manuf.* **2020**, *48*, 43.

[14] Y. Ling, W. Pang, X. Li, S. Goswami, Z. Xu, D. Stroman, Y. Liu, Q. Fei, Y. Xu, G. Zhao, B. Sun, J. Xie, G. Huang, Y. Zhang, Z. Yan, *Adv. Mater.* **2020**, *32*, 1908475.

[15] Y. Zhang, N. Zhang, H. Hingorani, N. Ding, D. Wang, C. Yuan, B. Zhang, G. Gu, Q. Ge, *Adv. Funct. Mater.* **2019**, *29*, 1806698.

[16] C. Yang, W. Wang, C. Yao, R. Xie, X.-J. Ju, Z. Liu, L.-Y. Chu, *Sci. Rep.* **2015**, *5*, 13622.

[17] Y. Yan, T. Santaniello, L. G. Bettini, C. Minnai, A. Bellacicca, R. Porotti, I. Denti, G. Faraone, M. Merlini, C. Lenardi, P. Milani, *Adv. Mater.* **2017**, *29*, 1606109.

[18] M. M. Hamedi, V. E. Campbell, P. Rothemund, F. Güder, D. C. Christodouleas, J. F. Bloch, G. M. Whitesides, *Adv. Funct. Mater.* **2016**, *26*, 2446.

[19] S. Yun, S. Park, B. Park, S. Ryu, S. M. Jeong, K. U. Kyung, *IEEE Trans. Ind. Electron.* **2020**, *67*, 717.

[20] J. Jeong, I. Bin Yasir, J. Han, C. H. Park, S.-K. Bok, K.-U. Kyung, *Appl. Sci.* **2019**, *9*, 4025.

[21] S. Mun, S. Yun, S. Nam, S. K. Park, S. Park, B. J. Park, J. M. Lim, K. U. Kyung, *IEEE Trans. Haptics* **2018**, *11*, 15.

[22] E. Sachyani Keneth, G. Scalet, M. Layani, G. Tibi, A. Degani, F. Auricchio, S. Magdassi, *Soft Rob.* **2020**, *7*, 123.

[23] X. L. Chang, P. S. Chee, E. H. Lim, R. C. C. Tan, *Smart Mater. Struct.* **2019**, *28*, 115011.

[24] Y.-C. Sun, B. D. Leaker, J. E. Lee, R. Nam, H. E. Naguib, *Sci. Rep.* **2019**, *9*, 11445.

[25] D. Pyo, S. Ryu, K. U. Kyung, S. Yun, D. S. Kwon, *Appl. Phys. Lett.* **2018**, *112*, 133902.

[26] S. Nam, S. Yun, J. W. Yoon, S. Park, S. K. Park, S. Mun, B. Park, K. U. Kyung, *Soft Rob.* **2018**, *5*, 777.

[27] J.-H. Youn, S. M. Jeong, G. Hwang, H. Kim, K. Hyeon, J. Park, K.-U. Kyung, *Appl. Sci.* **2020**, *10*, 640.

[28] A. Zolfagharian, A. Kaynak, S. Y. Khoo, A. Z. Kouzani, *3D Print. Addit. Manuf.* **2018**, *5*, 138.

[29] M.-Y. Choi, Y. Shin, H. S. Lee, S. Y. Kim, J.-H. Na, *Sci. Rep.* **2020**, *10*, 2482.

[30] Z. Sun, L. Yang, J. Zhao, W. Song, *J. Electrochem. Soc.* **2020**, *167*, 047515.

[31] Q. Shen, T. Wang, J. Liang, L. Wen, *Smart Mater. Struct.* **2013**, *22*, 075035.

[32] X. L. Chang, P. S. Chee, E. H. Lim, W. C. Chong, *Smart Mater. Struct.* **2019**, *28*, 015024.

[33] H. Lee, H. Kim, I. Ha, J. Jung, P. Won, H. Cho, J. Yeo, S. Hong, S. Han, J. Kwon, K. J. Cho, S. H. Ko, *Soft Rob.* **2019**, *6*, 760.

[34] Q. Li, X. Wang, L. Dong, C. Liu, S. Fan, *Soft Matter* **2019**, *15*, 9788.

[35] Y. Cao, J. Dong, *Sens. Actuators, A* **2019**, *297*, 111546.

[36] L. Yang, K. Qi, L. Chang, A. Xu, Y. Hu, H. Zhai, P. Lu, *J. Mater. Chem. B* **2018**, *6*, 5031.

[37] E. Sachyani, M. Layani, G. Tibi, T. Avidan, A. Degani, S. Magdassi, *Sens. Actuators, B* **2017**, *252*, 1071.

[38] Q. Wang, Y.-T. Li, T.-Y. Zhang, D.-Y. Wang, Y. Tian, J.-C. Yan, H. Tian, Y. Yang, F. Yang, T.-L. Ren, *Appl. Phys. Lett.* **2018**, *112*, 133902.

[39] Z. Xu, C. Ding, D. W. Wei, R. Y. Bao, K. Ke, Z. Liu, M. B. Yang, W. Yang, *ACS Appl. Mater. Interfaces* **2019**, *11*, 30332.

[40] T. Mu, L. Liu, X. Lan, Y. Liu, J. Leng, *Compos. Sci. Technol.* **2018**, *160*, 169.

[41] X. Gong, L. Liu, Y. Liu, J. Leng, *Smart Mater. Struct.* **2016**, *25*, 035036.

[42] F. P. Du, E. Z. Ye, W. Yang, T. H. Shen, C. Y. Tang, X. L. Xie, X. P. Zhou, W. C. Law, *Composites, Part B* **2015**, *68*, 170.

[43] K. Takashima, K. Sugitani, N. Morimoto, S. Sakaguchi, T. Noritsugu, T. Mukai, *Smart Mater. Struct.* **2014**, *23*, 125005.

[44] J. Biggs, K. Danielmeier, J. Hitzbleck, J. Krause, T. Kridl, S. Nowak, E. Orselli, X. Quan, D. Schapeler, W. Sutherland, J. Wagner, *Angew. Chem., Int. Ed.* **2013**, *52*, 9409.

[45] S. Rosset, H. R. Shea, *Appl. Phys. A: Mater. Sci. Process.* **2013**, *110*, 281.

[46] F. B. Madsen, A. E. Daugaard, S. Hvilsted, A. L. Skov, *Macromol. Rapid Commun.* **2016**, *37*, 378.

[47] H. Palza, P. Zapata, C. Angulo-Pineda, *Materials* **2019**, *12*, 277.

[48] J. Shang, X. Le, J. Zhang, T. Chen, P. Theato, *Polym. Chem.* **2019**, *10*, 1036.

[49] A. Minaminosono, H. Shigemune, Y. Okuno, T. Katsumata, N. Hosoya, S. Maeda, *Front. Robot. AI* **2019**, *6*, 1.

[50] C.-T. Chen, R.-C. Peng, *Smart Mater. Struct.* **2021**, *30*, 075010.

[51] H. Zhao, A. M. Hussain, M. Duduta, D. M. Vogt, R. J. Wood, D. R. Clarke, *Adv. Funct. Mater.* **2018**, *28*, 1804328.

[52] J. Meng, Y. Qiu, C. Hou, Q. Zhang, Y. Li, H. Wang, *Sens. Actuators, A* **2021**, *330*, 112889.

[53] G.-Y. Gu, J. Zhu, L.-M. Zhu, X. Zhu, *Bioinspir. Biomim.* **2017**, *12*, 011003.

[54] J. P. L. Bigué, J. S. Plante, *IEEE ASME Trans. Mechatron* **2013**, *18*, 169.

[55] M. Duduta, E. Hajiesmaili, H. Zhao, R. J. Wood, D. R. Clarke, *Proc. Natl. Acad. Sci. USA* **2019**, *116*, 2476.

[56] S. Rosset, H. R. Shea, *Appl. Phys. Rev.* **2016**, *3*, 031105.

[57] R. Pelrine, R. Kornbluh, Q. Pei, J. Joseph, *Science* **2000**, *287*, 836.

[58] J. S. Plante, S. Dubowsky, *Int. J. Solids Struct.* **2006**, *43*, 7727.

[59] S. J. A. Koh, T. Li, J. Zhou, X. Zhao, W. Hong, J. Zhu, Z. Suo, *J. Polym. Sci., Part B: Polym. Phys.* **2011**, *49*, 504.

[60] T. Lu, C. Ma, T. Wang, B. Li, H. Chen, J. Qiang, S. Hu, Z. Zhu, Y. Wang, S. J. A. Koh, T. Li, J. Zhou, X. Zhao, W. Hong, J. Zhu, Z. Suo, *J. Phys. D: Appl. Phys.* **2011**, *38*, 100752.

[61] L. Jiang, A. Betts, D. Kennedy, S. Jerrams, *J. Phys. D: Appl. Phys.* **2016**, *49*, 265401.

[62] S. Zakaria, P. H. F. Morshuis, M. Y. Benslimane, L. Yu, A. L. Skov, *Smart Mater. Struct.* **2015**, *24*, 055009.

[63] G. Kofod, *J. Phys. D: Appl. Phys.* **2008**, *41*, 215405.

[64] B. Li, H. Chen, J. Qiang, S. Hu, Z. Zhu, Y. Wang, *J. Phys. D: Appl. Phys.* **2011**, *44*, 155301.

[65] T. Lu, C. Ma, T. Wang, *Extreme Mech. Lett.* **2020**, *38*, 100752.

[66] M. Giousouf, G. Kovacs, *Smart Mater. Struct.* **2013**, *22*, 104010.

[67] M. Matysek, P. Lotz, K. Flittner, H. F. Schlaak, *Proc. SPIE* **2008**, *6927*, 692722.

[68] S. Reitelshöfer, M. Göttler, P. Schmidt, P. Treffer, M. Landgraf, J. Franke, *Proc. SPIE* **2016**, *9798*, 97981Y.

[69] G. Kovacs, L. Düring, S. Michel, G. Terrasi, *Sens. Actuators, A* **2009**, *155*, 299.

[70] A. Poulin, S. Rosset, H. R. Shea, *Appl. Phys. Lett.* **2015**, *107*, 244104.

[71] S. Taccola, A. Bellacicca, P. Milani, L. Beccai, F. Greco, *J. Appl. Phys.* **2018**, *124*, 064901.

[72] X. Ji, A. El Haitami, F. Sorba, S. Rosset, G. T. M. Nguyen, C. Plesse, F. Vidal, H. R. Shea, S. Cantin, *Sens. Actuators, B* **2018**, *261*, 135.

[73] X. Ji, X. Liu, V. Cacucciolo, M. Imboden, Y. Civet, A. El Haitami, S. Cantin, Y. Perriard, H. Shea, *Sci. Rob.* **2019**, *4*, aaz6451.

[74] D. M. Opris, *Adv. Mater.* **2018**, *30*, 1703678.

[75] J. Huang, F. Wang, L. Ma, Z. Zhang, E. Meng, C. Zeng, H. Zhang, D. Guo, *Chem. Eng. J.* **2022**, *428*, 131354.

[76] E. Acome, S. K. Mitchell, T. G. Morrissey, M. B. Emmett, C. Benjamin, M. King, M. Radakovitz, C. Keplinger, *Science* **2018**, *359*, 61.

[77] L. Duan, J. C. Lai, C. H. Li, J. L. Zuo, *ACS Appl. Mater. Interfaces* **2020**, *12*, 44137.

[78] Y. Zhang, C. Ellingford, R. Zhang, J. Roscow, M. Hopkins, P. Keogh, T. McNally, C. Bowen, C. Wan, *Adv. Funct. Mater.* **2019**, *29*, 1808431.

[79] C. H. Li, C. Wang, C. Keplinger, J. L. Zuo, L. Jin, Y. Sun, P. Zheng, Y. Cao, F. Lissel, C. Linder, X. Z. You, Z. Bao, *Nat. Chem.* **2016**, *8*, 618.

[80] A. Chortos, E. Hajiesmaili, J. Morales, D. R. Clarke, J. A. Lewis, *Adv. Funct. Mater.* **2020**, *30*, 1907375.

[81] X. Duan, J. Yu, Y. Zhu, Z. Zheng, Q. Liao, Y. Xiao, Y. Li, Z. He, Y. Zhao, H. Wang, L. Qu, *ACS Nano* **2020**, *14*, 14929.

[82] Y. Shin, M. Y. Choi, J. Choi, J. H. Na, S. Y. Kim, *ACS Appl. Mater. Interfaces* **2021**, *13*, 15633.

[83] H. Jiang, L. Fan, S. Yan, F. Li, H. Li, J. Tang, *Nanoscale* **2019**, *11*, 2231.

[84] K. Rotjanasuworapong, N. Thummarungsan, W. Lerdwijitjarud, A. Sirivat, *Carbohydr. Polym.* **2020**, *247*, 116709.

[85] Y. Cheng, X. Luo, J. Betz, S. Buckhout-White, O. Bekdash, G. F. Payne, W. E. Bentley, G. W. Rubloff, *Soft Matter* **2010**, *6*, 3177.

[86] A. Zolfagharian, A. Z. Kouzani, S. Y. Khoo, B. Nasri-Nasrabadi, A. Kaynak, *Sens. Actuators, A* **2017**, *265*, 94.

[87] D. Han, C. Farino, C. Yang, T. Scott, D. Browe, W. Choi, J. W. Freeman, H. Lee, *ACS Appl. Mater. Interfaces* **2018**, *10*, 17512.

[88] C. Yang, Z. Liu, C. Chen, K. Shi, L. Zhang, X. J. Ju, W. Wang, R. Xie, L. Y. Chu, *ACS Appl. Mater. Interfaces* **2017**, *9*, 15758.

[89] G. H. Kwon, Y. Y. Choi, J. Y. Park, D. H. Woo, K. B. Lee, J. H. Kim, S. H. Lee, *Lab Chip* **2010**, *10*, 1604.

[90] L. Ionov, *Adv. Funct. Mater.* **2013**, *23*, 4555.

[91] D. Morales, E. Palleau, M. D. Dickey, O. D. Velev, *Soft Matter* **2014**, *10*, 1337.

[92] T. Santaniello, L. Migliorini, E. Locatelli, I. Monaco, Y. Yan, C. Lenardi, M. Comes Franchini, P. Milani, *Smart Mater. Struct.* **2017**, *26*, 085030.

**ADVANCED
SCIENCE NEWS**

www.advancedsciencenews.com

**ADVANCED
MATERIALS
TECHNOLOGIES**

www.advmattechnol.de

[93] Y. Li, Y. Sun, Y. Xiao, G. Gao, S. Liu, J. Zhang, J. Fu, *ACS Appl. Mater. Interfaces* **2016**, *8*, 26326.

[94] *Bioinspired Sensing, Actuation, and Control in Underwater Soft Robotic Systems* (Eds: D. A. Paley, N. M. Wereley), Springer International Publishing, Cham **2021**.

[95] A. Khan, Inamuddin, R. K. Jain, M. Luqman, A. M. Asiri, *Sens. Actuators, A* **2018**, *280*, 114.

[96] C. Jo, D. Pugal, I. K. Oh, K. J. Kim, K. Asaka, *Prog. Polym. Sci.* **2013**, *38*, 1037.

[97] V. Panwar, C. Lee, S. Y. Ko, J. O. Park, S. Park, *Mater. Chem. Phys.* **2012**, *135*, 928.

[98] L. Yang, D. Zhang, X. Zhang, A. Tian, Y. Ding, *Int. J. Smart Nano Mater.* **2020**, *11*, 117.

[99] S. N. Akhtar, J. Cherusseri, J. Ramkumar, K. K. Kar, in *Composite Materials*, Springer Berlin Heidelberg, Berlin, Heidelberg **2017**, pp. 223–249.

[100] J. W. Lee, S. M. Hong, J. Kim, C. M. Koo, *Sens. Actuators, B* **2012**, *162*, 369.

[101] O. Kim, T. J. Shin, M. J. Park, *Nat. Commun.* **2013**, *4*, 2208.

[102] X. L. Wang, I. K. Oh, J. Lu, J. Ju, S. Lee, *Mater. Lett.* **2007**, *61*, 5117.

[103] A. Khan, Inamuddin, R. K. Jain, M. Naushad, *RSC Adv.* **2015**, *5*, 91564.

[104] Inamuddin, A. Khan, M. Luqman, A. Dutta, *Sens. Actuators, A* **2014**, *216*, 295.

[105] V. Palmre, D. Pugal, K. J. Kim, K. K. Leang, K. Asaka, A. Aabloo, *Sci. Rep.* **2015**, *4*, 6176.

[106] D. Guo, L. Wang, X. Wang, Y. Xiao, C. Wang, L. Chen, Y. Ding, *Sens. Actuators, B* **2020**, *305*, 127488.

[107] B. Xu, S. Wang, Z. Zhang, J. Ling, X. Wu, *Sci. Rep.* **2021**, *11*, 7639.

[108] A. Potekhina, C. H. Wang, *Actuators* **2019**, *8*, 69.

[109] Y. Tian, Y. T. Li, H. Tian, Y. Yang, T. L. Ren, *Soft Rob.* **2021**, *8*, 241.

[110] G. Tibi, E. Sachyani Keneth, M. Layani, S. Magdassi, A. Degani, *Soft Rob.* **2020**, *7*, 649.

[111] Y. Zhu, M. Birla, K. R. Oldham, E. T. Filipov, *Adv. Funct. Mater.* **2020**, *30*, 2003741.

[112] M. Sang, G. Liu, S. Liu, Y. Wu, S. Xuan, S. Wang, S. Xuan, W. Jiang, X. Gong, *Chem. Eng. J.* **2021**, *414*, 128883.

[113] S. Yao, J. Cui, Z. Cui, Y. Zhu, *Nanoscale* **2017**, *9*, 3797.

[114] J. Ahn, Y. Jeong, Z. Zhao, S. Hwang, K. Kim, J. Ko, S. Jeon, J. Park, H. Kang, J. Jeong, I. Park, *Adv. Mater. Technol.* **2020**, *5*, 1900997.

[115] J. Zhu, M. Cho, Y. Li, T. He, J. Ahn, J. Park, T. L. Ren, C. Lee, I. Park, *Nano Energy* **2021**, *86*, 106035.

[116] Y. Jeong, J. Gu, J. Byun, J. Ahn, J. Byun, K. Kim, J. Park, J. Ko, J. Jeong, M. Amjadi, I. Park, *Adv. Healthcare Mater.* **2021**, *10*, 2001461.

[117] Y. Jeong, H. jung Kang, Z. jun Zhao, J. Ahn, S. Hyoung Hwang, S. Jeon, J. Ko, J. Y. Jung, I. Park, J. ho Jeong, *Appl. Surf. Sci.* **2021**, *552*, 149500.

[118] J. Ahn, Z. J. Zhao, J. Choi, Y. Jeong, S. Hwang, J. Ko, J. Gu, S. Jeon, J. Park, M. Kang, D. V. Del Orbe, I. Cho, H. Kang, M. Bok, J. H. Jeong, I. Park, *Nano Energy* **2021**, *85*, 105978.

[119] J. Gu, J. Ahn, J. Jung, S. Cho, J. Choi, Y. Jeong, J. Park, S. Hwang, I. Cho, J. Ko, J.-H. Ha, Z.-J. Zhao, S. Jeon, S. Ryu, J.-H. Jeong, I. Park, *Nano Energy* **2021**, *89*, 106447.

[120] J. Gu, D. Kwon, I. Park, in *2018 IEEE Micro Electro Mechanical Systems (MEMS)*, IEEE, Belfast, UK **2018**, pp. 889–892.

[121] J. Gu, D. Kwon, J. Ahn, I. Park, in *2019 20th International Conference on Solid-State Sensors, Actuators and Microsystems & Eurosensors XXXIII (TRANSDUCERS & EUROSENSORS XXXIII)*, IEEE, Berlin, Germany **2019**, pp. 1716–1719.

[122] J. Ahn, J. Gu, Y. Jeong, K. Kim, J. Jeong, I. Park, in *2019 IEEE 32nd International Conference on Micro Electro Mechanical Systems (MEMS)*, IEEE, Seoul, Korea **2019**, pp. 303–306.

[123] J. Gu, D. Kwon, J. Ahn, I. Park, *ACS Appl. Mater. Interfaces* **2020**, *12*, 10908.

[124] J. Choi, D. Kwon, K. Kim, J. Park, D. Del Orbe, J. Gu, J. Ahn, I. Cho, Y. Jeong, Y. Oh, I. Park, *ACS Appl. Mater. Interfaces* **2020**, *12*, 1698.

[125] J. Choi, D. Kwon, B. Kim, K. Kang, J. Gu, J. Jo, K. Na, J. Ahn, D. Del Orbe, K. Kim, J. Park, J. Shim, J. Y. Lee, I. Park, *Nano Energy* **2020**, *74*, 104749.

[126] Y. Jeong, J. Park, J. Lee, K. Kim, I. Park, *ACS Sens.* **2020**, *5*, 481.

[127] Z.-J. Zhao, J. Ko, J. Ahn, M. Bok, M. Gao, S. H. Hwang, H.-J. Kang, S. Jeon, I. Park, J.-H. Jeong, *ACS Sens.* **2020**, *5*, 2367.

[128] K. Hwang, J. Ahn, I. Cho, K. Kang, K. Kim, J. Choi, K. Polychronopoulou, I. Park, *ACS Appl. Mater. Interfaces* **2020**, *12*, 13338.

[129] J. Ko, Z. J. Zhao, S. H. Hwang, H. J. Kang, J. Ahn, S. Jeon, M. Bok, Y. Jeong, K. Kang, I. Cho, J. H. Jeong, I. Park, *ACS Nano* **2020**, *14*, 2191.

[130] H. Kim, H. Lee, I. Ha, J. Jung, P. Won, H. Cho, J. Yeo, S. Hong, S. Han, J. Kwon, K.-J. Cho, S. H. Ko, *Adv. Funct. Mater.* **2018**, *28*, 1801847.

[131] Q. Ji, Z. Jing, J. Shen, Y. Hu, L. Chang, L. Lu, M. Liu, J. Liu, Y. Wu, *Adv. Intell. Syst.* **2021**, *3*, 2000240.

[132] M. Amjadi, M. Sitti, *ACS Nano* **2016**, *10*, 10202.

[133] M. Amjadi, M. Sitti, *Adv. Sci.* **2018**, *5*, 1800239.

[134] J. Li, L. Mou, R. Zhang, J. Sun, R. Wang, B. An, H. Chen, K. Inoue, R. Ovalle-Robles, Z. Liu, *Carbon* **2019**, *148*, 487.

[135] L. Chen, M. Weng, P. Zhou, F. Huang, C. Liu, S. Fan, W. Zhang, *Adv. Funct. Mater.* **2019**, *29*, 1806057.

[136] Q. Li, C. Liu, S. Fan, *Nanotechnology* **2018**, *29*, 175503.

[137] Q. Wang, Y. T. Li, T. Y. Zhang, D. Y. Wang, Y. Tian, J. C. Yan, H. Tian, Y. Yang, F. Yang, T. L. Ren, *Appl. Phys. Lett.* **2018**, *112*, 133902.

[138] C. Wang, M. Wang, S. Ying, J. Gu, *Macromol. Mater. Eng.* **2020**, *305*, 1900602.

[139] C. Chu, Z. Xiang, J. Wang, H. Xie, T. Xiang, S. Zhou, *J. Mater. Chem. B* **2020**, *8*, 8061.

[140] K. K. Patel, R. Purohit, *Mater. Today Commun.* **2019**, *20*, 100579.

[141] Q. Ze, X. Kuang, S. Wu, J. Wong, S. M. Montgomery, R. Zhang, J. M. Kovitz, F. Yang, H. J. Qi, R. Zhao, *Adv. Mater.* **2020**, *32*, 1906657.

[142] W. Miao, W. Zou, B. Jin, C. Ni, N. Zheng, Q. Zhao, T. Xie, *Nat. Commun.* **2020**, *11*, 4257.

[143] Y. Chen, Y. Chen, H. U. Rehman, X. Zheng, H. Li, H. Liu, M. S. Hedenqvist, *Molecules* **2020**, *25*, 4246.

[144] C. S. Haines, M. D. Lima, N. Li, G. M. Spinks, J. Foroughi, J. D. W. Madden, S. H. Kim, S. Fang, M. J. De Andrade, F. Göktepe, Ö. Göktepe, S. M. Mirvakili, S. Naficy, X. Lepró, J. Oh, M. E. Kozlov, S. J. Kim, X. Xu, B. J. Swedlove, G. G. Wallace, R. H. Baughman, *Science* **2014**, *343*, 868.

[145] S.-t. Xing, P.-p. Wang, S.-q. Liu, Y.-h. Xu, R.-m. Zheng, Z.-f. Deng, Z.-f. Peng, J.-y. Li, Y.-y. Wu, L. Liu, *Compos. Sci. Technol.* **2020**, *193*, 108133.

[146] P. Yang, G. Zhu, X. Shen, X. Yan, J. Nie, *RSC Adv.* **2016**, *6*, 90212.

[147] J. J. Song, H. H. Chang, H. E. Naguib, *Eur. Polym. J.* **2015**, *67*, 186.

[148] H. Xie, L. Li, X. Y. Deng, C. Y. Cheng, K. K. Yang, Y. Z. Wang, *Compos. Sci. Technol.* **2018**, *157*, 202.

[149] W. Wang, Y. Liu, J. Leng, *Coord. Chem. Rev.* **2016**, *320–321*, 38.

[150] Q. Peng, H. Wei, Y. Qin, Z. Lin, X. Zhao, F. Xu, J. Leng, X. He, A. Cao, Y. Li, *Nanoscale* **2016**, *8*, 18042.

[151] B. Aksoy, N. Besse, R. J. Boom, B. J. Hoogenberg, M. Blom, H. Shea, *Lab Chip* **2019**, *19*, 608.

[152] J. Shintake, S. Rosset, B. Schubert, D. Floreano, H. Shea, *Adv. Mater.* **2016**, *28*, 231.

[153] N. Kellaris, V. Gopaluni Venkata, G. M. Smith, S. K. Mitchell, C. Keplinger, *Sci. Rob.* **2018**, *3*, aar3276.

[154] D. Kim, S. Song, S. Jang, G. Kim, J. Lee, Y. Lee, S. Park, *Smart Mater. Struct.* **2020**, *29*, 085024.

[155] D. Li, D. Niu, G. Ye, B. Lei, J. Han, W. Jiang, F. Luo, J. Chen, H. Liu, B. Lu, *Appl. Mater. Today* **2021**, *24*, 101091.

[156] S. Pfeil, M. Henke, K. Katzer, M. Zimmermann, G. Gerlach, *Front. Rob. AI* **2020**, *7*, 1.

[157] J. Najem, S. A. Sarles, B. Akle, D. J. Leo, *Smart Mater. Struct.* **2012**, *21*, 094026.

2200041 (19 of 21)

**ADVANCED
SCIENCE NEWS**

www.advancedsciencenews.com

**ADVANCED
MATERIALS
TECHNOLOGIES**

www.advmattechnol.de

[158] Z. Chen, T. I. Um, H. Bart-Smith, *Int. J. Smart Nano Mater.* **2012**, *3*, 296.

[159] M. Philen, W. Neu, *Smart Mater. Struct.* **2011**, *20*, 094015.

[160] J.-H. Youn, K. Hyeon, J. H. Ma, K.-U. Kyung, *Smart Mater. Struct.* **2019**, *28*, 124001.

[161] J. Li, Y. Wang, L. Liu, S. Xu, Y. Liu, J. Leng, S. Cai, *Adv. Funct. Mater.* **2019**, *29*, 1903762.

[162] L. Maffli, S. Rosset, M. Ghilardi, F. Carpi, H. Shea, *Adv. Funct. Mater.* **2015**, *25*, 1656.

[163] S. Park, B. Park, S. Nam, S. Yun, S. K. Park, S. Mun, J. M. Lim, Y. Ryu, S. H. Song, K.-U. Kyung, *Opt. Express* **2017**, *25*, 23801.

[164] Q. Liu, J. Zuo, C. Zhu, S. Q. Xie, *Future Gener. Comput. Syst.* **2020**, *113*, 620.

[165] M. Pan, C. Yuan, X. Liang, T. Dong, T. Liu, J. Zhang, J. Zou, H. Yang, C. Bowen, *Adv. Intell. Syst.* **2021**, *4*, 2100140.

[166] A. S. Arockia Doss, H. Sharma, *Advances in Robotics –5th Int. Conf. of The Robotics Society*, ACM, New York, NY **2021**, pp. 1–6.

[167] Y. Li, M. Hashimoto, *Smart Mater. Struct.* **2017**, *26*, 125003.

[168] M. Duduta, E. Hajiesmaili, H. Zhao, R. J. Wood, D. R. Clarke, *Proc. Natl. Acad. Sci. USA* **2019**, *116*, 2476.

[169] A. Behboodi, C. DeSantis, J. Lubsen, S. C. K. Lee, in *2020 42nd Annual International Conference of the IEEE Engineering in Medicine & Biology Society (EMBC)*, IEEE, Montreal, QC, Canada **2020**, pp. 4930–4935.

[170] Ankit, T. Y. K. Ho, A. Nirmal, M. R. Kulkarni, D. Accoto, N. Mathews, *Adv. Intell. Syst.* **2022**, *4*, 2100061.

[171] Ankit, N. Tiwari, M. Rajput, N. A. Chien, N. Mathews, *Small* **2018**, *14*, 1702312.

[172] E. Leroy, R. Hinchet, H. Shea, *Adv. Mater.* **2020**, *32*, 2002564.

[173] G. H. Feng, S. Y. Hou, *Sens. Actuators, A* **2018**, *275*, 137.

[174] S. J. Kim, D. Pugal, J. Wong, K. J. Kim, W. Yim, *Rob. Auton. Syst.* **2014**, *62*, 53.

[175] Z. Peng, Y. Shi, N. Chen, Y. Li, Q. Pei, *Adv. Funct. Mater.* **2021**, *31*, 2008321.

Junseong Ahn is a Ph.D. candidate at the Korea Advanced Institute of Science and Technology (KAIST). He received his M.S. degree at KAIST in 2019. His current research interest is focused on micro/nanostructuring, and their application to sensors, actuators, and energy harvesting devices.

Jimin Gu is a Ph.D. candidate at the Korea Advanced Institute of Science and Technology (KAIST). She received her M.S. degree at KAIST in 2019. Her current research interest is focused on soft sensors and stretchable electronics for biomedical and healthcare applications.

Jungrak Choi is a Ph.D. candidate at the Korea Advanced Institute of Science and Technology (KAIST). He received his M.S. degree at KAIST and Technical University of Denmark (DTU) in 2018. His current research interest is focused on customizable 3D electronics based on thermoforming.

**ADVANCED
SCIENCE NEWS**

www.advancedsciencenews.com

**ADVANCED
MATERIALS
TECHNOLOGIES**

www.advmattechnol.de

Morteza Amjadi is an Assistant Professor of Mechanical Engineering at Heriot-Watt University, UK. He received his B.Sc. and M.Sc. degrees from Iran University of Science and Technology (IUST) and Korea Advanced Institute of Science and Technology (KAIST) in 2012 and 2014, respectively, and his D.Sc. degree jointly from Max Planck Institute for Intelligent Systems and ETH Zurich. His research interests include wearable medical devices, smart materials, composites, and soft robotics.

Inkyu Park received his B.S., M.S., and Ph.D. from KAIST (1998), UIUC (2003), and UC Berkeley (2007), respectively, all in mechanical engineering. He has been with the department of mechanical engineering at KAIST since 2009 as a faculty member and is currently a full professor and a KAIST Endowed Chair Professor. His research interests are nanofabrication, smart sensors for healthcare, environmental and biomedical monitoring, nanomaterial-based sensors and flexible and wearable electronics. He is a recipient of HP Open Innovation Research Award (2009–2012), KAIST Endowed Chair Professorship (2017), and Outstanding Researcher Award from the MNS Society of Korea (2020; 2022).